Analysis of lattice Boltzmann methods

Regular and multiscale expansions

Short course material – ICMMES 2006, Hampton(Virginia)

Michael Junk and Martin Rheinländer

2nd October 2006

Contents

1 Introduction **1**

2 The lattice Boltzmann algorithm **2**
2.1 A few words concerning the notation 2
2.2 Presentation of the algorithm 3

3 Regular expansion **4**
3.1 Analysis of the update rule 4
3.2 Analysis of initial conditions 11
3.3 Consistency 13
3.4 Explicit computation of the mass moments 15

4 Multiscale Expansion **17**
4.1 A numerical experiment to detect different time scales 17
4.2 Additional quadratic time scale 21
4.3 Additional cubic time scale 25

5 Appendix **29**

1 Introduction

In this course we focus on the analysis of lattice Boltzmann schemes by asymptotic methods. Since asymptotic analysis lives mainly by concrete case studies rather than by collections of abstract recipes, we propose a simple lattice Boltzmann algorithm, which is used to develop and to illustrate the ideas simultaneously. In particular, the goal of our presentation is to answer (at least partly) the following questions:

- How to perform a consistency analysis of numerical schemes by *regular* expansions?

- Where are the shortcomings of regular expansions. For instance: Regular expansions may fail to reflect correctly the long term behavior of the scheme.
- What are *multiscale* expansions and how do they come naturally into play, to describe the numerical algorithms more accurately?

We stress that all methods presented here are not restricted to lattice Boltzmann methods but can readily be applied to any other finite difference scheme.

2 The lattice Boltzmann algorithm

2.1 A few words concerning the notation

Lattice Boltzmann methods are based on discrete velocity particle models. Concretely, we consider fictitious particles that can move with unit speed in one space dimension either to the left or to the right. Hence the discrete velocities are given by $\mathcal{S} := \{s_1, s_2\} = \{-1, 1\}$. The particle distribution is described by a vector-valued function referred to as the *population function*. The first component represents the density of the particles traveling to the left, while the second component is associated with the other species:

$$\mathsf{F}(t,x) = \big[\mathsf{F}_k(t,x)\big]_{k\in\{1,2\}} = \begin{pmatrix} \mathsf{F}_1(t,x) \\ \mathsf{F}_2(t,x) \end{pmatrix}.$$

Observe that the components, which we denote as *populations*, depend on time and space. In order to keep the conception[1] clear we designate $\mathbb{R}^2$ by $\mathbb{R}^{\mathcal{S}}$, if the indices refer to the discrete velocities. Elements of $\mathbb{R}^{\mathcal{S}}$ are highlighted by sans-serif characters. Let us introduce the following abbreviations, that will simplify the computations of later sections:

$$\mathsf{1} := \tbinom{1}{1} \in \mathbb{R}^{\mathcal{S}} \qquad \mathsf{s} := \tbinom{s_1}{s_2} = \tbinom{-1}{1} \in \mathbb{R}^{\mathcal{S}}$$

The scalar product in $\mathbb{R}^{\mathcal{S}}$ is indicated by brackets. In particular we have:

$$\langle \mathsf{f}, \mathsf{g} \rangle := \mathsf{f}_1\mathsf{g}_1 + \mathsf{f}_2\mathsf{g}_2 \quad \Rightarrow \quad \langle \mathsf{1}, \mathsf{1} \rangle = \langle \mathsf{s}, \mathsf{s} \rangle = 2 \quad \text{and} \quad \langle \mathsf{1}, \mathsf{s} \rangle = 0. \tag{1}$$

For $\mathsf{f} \in \mathbb{R}^{\mathcal{S}}$ we call the scalar products $\langle \mathsf{f}, \mathsf{1} \rangle$ and $\langle \mathsf{f}, \mathsf{s} \rangle$ *mass moment* (0^{th} moment) and *flux moment* (1^{st} moment) respectively. Furthermore, we will extensively make use of componentwise multiplication for $\mathsf{f}, \mathsf{g} \in \mathbb{R}^{\mathcal{S}}$:

$$\mathsf{gf} = \mathsf{fg} = \tbinom{\mathsf{f}_1}{\mathsf{f}_2}\tbinom{\mathsf{g}_1}{\mathsf{g}_2} := \tbinom{\mathsf{f}_1\mathsf{g}_1}{\mathsf{f}_2\mathsf{g}_2} \quad \Rightarrow \quad \mathsf{1f} = \mathsf{f}, \quad \mathsf{s}^2 = \begin{pmatrix} (-1)^2 \\ 1^2 \end{pmatrix} = \mathsf{1}, \quad \mathsf{s}^3 = \mathsf{s}\,.$$

By slight abuse[2] of notation, we understand the usually invalid operation $a + \mathsf{f}$ with $a \in \mathbb{R}$ and $\mathsf{f} \in \mathbb{R}^{\mathcal{S}}$ in the sense of $a + \mathsf{f} := a\mathsf{1} + \mathsf{f}$.

[1] In allusion to the *phase-space density* of the *Boltzmann equation*, it would be natural to describe the particle distribution with a function $(t, x, s) \mapsto \tilde{\mathsf{F}}(t, x, s)$ where the variable s can only take the two values s_1 and s_2. However, we abstain from this point of view, using the more familiar vector notation $\mathsf{F}_k(t, x) = \tilde{\mathsf{F}}(t, x, s_k)$ instead.

[2] A reader familiar with MATLAB may notice the analogy with respect to the componentwise multiplication operator (`.*`) for matrices as well as the addition of scalars and matrices.

2.2 Presentation of the algorithm

The algorithm we are going to investigate has the standard lattice Boltzmann form

$$\mathsf{F}_k(t+h, x+s_k h) = \mathsf{F}_k(t,x) + \big[J\mathsf{F}(t,x)\big]_k, \qquad k = 1,2 \tag{2}$$

where the discretization parameter $h = 1/N$, $N \in \mathbb{N}$ determines the space-time grid. More precisely, t can take the values $t_n = nh$ with $n \in \mathbb{N}_0$ and x ranges in $x_i = ih$ with $i \in \mathbb{Z}$. The collision operator J on the right hand side of (2) models the particle interaction. Here, we choose the simple BGK form

$$J\mathsf{F} = \omega(\mathsf{E}(U) - \mathsf{F})$$

with relaxation parameter ω. The equilibrium distribution $\mathsf{E}(U)$ is assumed to depend only on the mass moment U of F

$$\mathsf{E}(U) := \tfrac{1}{2}(1 + a\mathsf{s})U, \qquad U = \langle \mathsf{F}, 1\rangle.$$

The role of the parameter $a \in \mathbb{R}$ will be explained later. In view of (1) we observe that

$$\langle \mathsf{E}(U), 1\rangle = \tfrac{1}{2}U\langle 1, 1\rangle + \tfrac{1}{2}aU\langle \mathsf{s}, 1\rangle = U$$

so that

$$\langle J\mathsf{F}, 1\rangle = \omega\left\langle \mathsf{E}\big(\langle \mathsf{F}, 1\rangle\big), 1\right\rangle - \omega\langle \mathsf{F}, 1\rangle = \omega\langle \mathsf{F}, 1\rangle - \omega\langle \mathsf{F}, 1\rangle = 0$$

which expresses the mass conservation during the collision process. We remark that the collision operator is linear in our example because the equilibrium distribution depends linearly on F. In fact, we can write for a general $\mathsf{f} \in \mathbb{R}^{\mathcal{S}}$

$$\begin{aligned}\mathsf{E}_1(\langle \mathsf{f}, 1\rangle) &= \tfrac{1}{2}(1 + as_1)\langle \mathsf{f}, 1\rangle = \tfrac{1}{2}(1-a)\mathsf{f}_1 + \tfrac{1}{2}(1-a)\mathsf{f}_2\\ \mathsf{E}_2(\langle \mathsf{f}, 1\rangle) &= \tfrac{1}{2}(1 + as_2)\langle \mathsf{f}, 1\rangle = \tfrac{1}{2}(1+a)\mathsf{f}_1 + \tfrac{1}{2}(1+a)\mathsf{f}_2\end{aligned}$$

so that $\mathsf{E}(\langle \mathsf{f}, 1\rangle) = E\mathsf{f}$ with the matrix

$$E := \tfrac{1}{2}\begin{pmatrix} 1-a & 1-a \\ 1+a & 1+a \end{pmatrix} \tag{3}$$

which satisfies the projector property $E = E^2$. Using this notation, the collision operator is given by the matrix $J = \omega(E - I)$ and the algorithm (2) appears in the form

$$\mathsf{F}_k(t+h, x+s_k h) = (1-\omega)\mathsf{F}_k(t,x) + \omega\big[E\mathsf{F}(t,x)\big]_k. \tag{4}$$

Apart from this update rule we require suitable initial and boundary conditions to fully specify the particle dynamics.
A typical initialization rule is based on the equilibrium distribution. Given some function $x \mapsto v_0(x)$, one may set

$$\mathsf{F}(0,x) = \mathsf{E}(v_0(x)). \tag{5}$$

Improvements of this basic rule will be derived in the sequel. In order to keep our first analysis as simple as possible, we assume that v_0 is a 1-periodic function, i.e. $v_0(x+1) = v_0(x)$. Since the grid points $x_i = ih = i/N$, $i \in \mathbb{Z}$ are compatible with

this periodicity in the sense that $x_i + 1 = x_{i+N}$, we can conclude that the lattice Boltzmann solution is also 1-periodic. In particular, it suffices to compute F only on the *finite* subset $\{x_0, \ldots, x_{N-1}\}$. The required information from the neighbors of the trailing points follows from periodicity

$$\mathsf{F}(t, x_{-1}) = \mathsf{F}(t, x_{N-1}), \qquad \mathsf{F}(t, x_N) = \mathsf{F}(t, x_0) \tag{6}$$

which can be regarded as a boundary condition.

3 Regular expansion

3.1 Analysis of the update rule

Implementing the lattice Boltzmann algorithm introduced above with initial value $v_0(x) = \cos(2\pi x)$, for example, we observe the following dynamics of $U = \langle \mathsf{F}, 1 \rangle$: provided $|a|$ is small enough (otherwise the algorithm is unstable), the initial cosine-shape of the graph moves with a speed related to the parameter a. Repeating the simulation with smaller grid size h, we observe similar profiles. It turns out that the amplitude of the cosine reduces during the movement and this reduction is more pronounced for larger values of h.

In order to understand the behavior of the lattice Boltzmann solution $\mathsf{F}(t, x)$ more thoroughly, we try to approximate it in the form of a regular h-expansion

$$\mathsf{F}(t, x) \approx \mathsf{f}^{[\alpha]}(t, x) := \mathsf{f}^{(0)}(t, x) + h\mathsf{f}^{(1)}(t, x) + \ldots + h^\alpha \mathsf{f}^{(\alpha)}(t, x) \tag{7}$$

with $t = t_n = nh$ and $x = x_j = jh$, $n \in \mathbb{N}, j \in \mathbb{Z}$. Note that $\mathsf{f}^{[\alpha]}$ is a polynomial[3] of order $\alpha \in \mathbb{N}$ with respect to the grid parameter h. We refer to $\mathsf{f}^{[\alpha]}$ as *prediction function*. The *asymptotic order functions* $\mathsf{f}^{(\beta)}$ with $0 \le \beta \le \alpha$ are supposed to be h-independent. Hence they are defined on the whole unit interval $[0, 1]$. In order to take the boundary conditions (6) of the algorithm into account, they should be extendible to smooth, 1-periodic functions on $\mathbb{R}$.

If the prediction function $\mathsf{f}^{[\alpha]}$ nicely approximates[4] the population function F for small h, then $\mathsf{f}^{[\alpha]}$ also satisfies the LB equation (4) up to a small residual. This observation leads to the rule to determine the coefficients $\mathsf{f}^{(\beta)}$: they are chosen in such a way that the residual has highest possible order in h and thus vanishes with optimal speed as h tends to zero. More specifically, we require for all $h > 0$

$$\mathsf{f}_k^{[\alpha]}(t + h, x + s_k h) = (1 - \omega)\mathsf{f}_k^{[\alpha]}(t, x) + \omega \big[E\mathsf{f}^{[\alpha]}(t, x)\big]_k \; + \; \mathrm{O}(h^{\alpha+1}). \tag{8}$$

Under the assumption that the asymptotic order functions are sufficiently smooth we substitute $\mathsf{f}_k^{[\alpha]}(t + h, x + s_k h)$ by its Taylor expansion around (t, x) up to the

[3] This particular h-dependence is motivated by the theorem of Weierstraß which states that the polynomials are dense in the space of continuous functions over a compact interval like $[0, 1]$. Hence any continuous function is arbitrarily well approximated by polynomials. This confirms, that the set of polynomials might be ample enough, to approximate the grid dependency of the population function F provided it behaves continuously in h.

[4] Strictly speaking the approximation refers to the restriction of $\mathsf{f}^{[\alpha]}$ onto the corresponding grid.

order α:

$$\mathsf{f}_k^{[\alpha]}(t+h, x+s_k h) = \sum_{\beta=0}^{\alpha} \tfrac{1}{\beta!} h^\beta \, (\, \partial_t + s_k \partial_x \,)^\beta \, \mathsf{f}_k^{[\alpha]}(t,x) \;+\; \mathrm{O}(h^{\alpha+1}). \tag{9}$$

A convenient effect of the Taylor expansion is, that it disentangles the index-depending spatial argument at the left hand side. Therefore we may now write vectors instead of components (i.e. f in place of f_k), such that equation (8) in combination with the Taylor expansion reads[5]

$$\sum_{\beta=0}^{\alpha} \tfrac{1}{\beta!} h^\beta \, (\underbrace{\partial_t + \mathsf{s}\partial_x}_{=:D})^\beta \, \mathsf{f}^{[\alpha]} = (1-\omega)\mathsf{f}^{[\alpha]} + \omega E \mathsf{f}^{[\alpha]} \;+\; \mathrm{O}(h^{\alpha+1}).$$

If we replace $\mathsf{f}^{[\alpha]}$ by the truncated series in (7) and incorporate those terms into $\mathrm{O}(h^{\alpha+1})$ that are proportional to some power of h with an exponent greater than α, we obtain

$$\sum_{\beta=0}^{\alpha} \sum_{\gamma=0}^{\beta} \tfrac{1}{\gamma!} h^\beta \; D^\gamma \; \mathsf{f}^{(\beta-\gamma)} = (1-\omega) \sum_{\beta=0}^{\alpha} h^\beta \mathsf{f}^{(\beta)} + \omega \sum_{\beta=0}^{\alpha} h^\beta E \mathsf{f}^{(\beta)} \;+\; \mathrm{O}(h^{\alpha+1}).$$

This equation, that shall hold true for arbitrary h, enforces the equality of the coefficients referring on both sides to the same powers of h. In particular the *comparison of coefficients* yields for $\alpha \geq 4$ and $0 \leq \beta \leq 4$:

$$\left.\begin{array}{lll}
h^0: & \mathsf{f}^{(0)} & = (1-\omega)\mathsf{f}^{(0)} + \omega E \mathsf{f}^{(0)} \\
h^1: & \mathsf{f}^{(1)} + D\mathsf{f}^{(0)} & = (1-\omega)\mathsf{f}^{(1)} + \omega E \mathsf{f}^{(1)} \\
h^2: & \mathsf{f}^{(2)} + D\mathsf{f}^{(1)} + \tfrac{1}{2} D^2 \mathsf{f}^{(0)} & = (1-\omega)\mathsf{f}^{(2)} + \omega E \mathsf{f}^{(2)} \\
h^3: & \mathsf{f}^{(3)} + D\mathsf{f}^{(2)} + \tfrac{1}{2} D^2 \mathsf{f}^{(1)} + \tfrac{1}{6} D^3 \mathsf{f}^{(0)} & = (1-\omega)\mathsf{f}^{(3)} + \omega E \mathsf{f}^{(3)} \\
h^4: & \mathsf{f}^{(4)} + D\mathsf{f}^{(3)} + \tfrac{1}{2} D^2 \mathsf{f}^{(2)} + \tfrac{1}{6} D^3 \mathsf{f}^{(1)} + \tfrac{1}{24} D^4 \mathsf{f}^{(0)} & = (1-\omega)\mathsf{f}^{(4)} + \omega E \mathsf{f}^{(4)}
\end{array}\right\} \tag{10}$$

Next, we gather in each equation the terms of highest index at the left hand side, while the other terms are collected at the right:

$$\left.\begin{array}{lll}
(I-E)\mathsf{f}^{(0)} &=& 0 \\
(I-E)\mathsf{f}^{(1)} &=& -\tfrac{1}{\omega} D\mathsf{f}^{(0)} \\
(I-E)\mathsf{f}^{(2)} &=& -\tfrac{1}{\omega} D\mathsf{f}^{(1)} - \tfrac{1}{2\omega} D^2 \mathsf{f}^{(0)} \\
(I-E)\mathsf{f}^{(3)} &=& -\tfrac{1}{\omega} D\mathsf{f}^{(2)} - \tfrac{1}{2\omega} D^2 \mathsf{f}^{(1)} - \tfrac{1}{6\omega} D^3 \mathsf{f}^{(0)} \\
(I-E)\mathsf{f}^{(4)} &=& -\tfrac{1}{\omega} D\mathsf{f}^{(3)} - \tfrac{1}{2\omega} D^2 \mathsf{f}^{(2)} - \tfrac{1}{6\omega} D^3 \mathsf{f}^{(1)} - \tfrac{1}{24\omega} D^4 \mathsf{f}^{(0)}
\end{array}\right\} \tag{11}$$

Obviously, we obtain for each asymptotic order function a linear equation with the common system matrix $I-E$. Furthermore the asymptotic order functions depend hierarchically on their "comrades" of lower order, which appear as inhomogeneities.

[5] We consider D as a special differentiation operator, therefore we should define it by $D := I\partial_t + S\partial_x$, where I is the 2×2 identity matrix and $S := \left(\begin{smallmatrix} -1 & 0 \\ 0 & 1 \end{smallmatrix}\right)$ Note that the matrix multiplication with I and D is equivalent to the vector multiplication with $\mathsf{1}$ and s respectively.

This implies that the equations must be solved successively starting with the homogeneous equation for $\mathsf{f}^{(0)}$. However, the singularity of $I-E$ seems to create a problem. In fact, we have

$$I-E=\begin{pmatrix}1&0\\0&1\end{pmatrix}-\tfrac{1}{2}\begin{pmatrix}1-a&1-a\\1+a&1+a\end{pmatrix}=\tfrac{1}{2}\begin{pmatrix}1+a&-1+a\\-1-a&1-a\end{pmatrix} \tag{12}$$

which shows that the rank of $I-E$ is only 1 (the rows differ only by sign). At first sight this seems to be disturbing, because the lack of an inverse matrix $(I-E)^{-1}$ entails, that the solution for arbitrary right hand sides may not exist or is not unique in the affirmative case. A second glance reveals, however, that the regular expansion ansatz would fail, if $I-E$ were invertible. In this case $\mathsf{f}^{(0)}$ could only be 0 yielding by induction 0 for all the other asymptotic order functions. So $\mathsf{f}^{[\alpha]}$ would have no other choice than to vanish thus trapping the ansatz into a *cul-de-sac*.
Let us now look under what circumstances the 2×2 system $(I-E)\mathsf{x}=\mathsf{y}$ has a solution. As the image space of $I-E$ is spanned[6] by s

$$\operatorname{image}(I-E)=\operatorname{span}\left\{\begin{pmatrix}-1\\1\end{pmatrix}\right\}=\operatorname{span}\{\mathsf{s}\},$$

the inhomogeneous equations admit only solutions for right hand sides being multiples of s. Since $\{\mathsf{1},\mathsf{s}\}$ forms an orthogonal basis in $\mathbb{R}^{\mathcal{S}}$ every vector and in particular y admits the representation

$$\mathsf{y}=\tfrac{1}{2}\langle\mathsf{y},\mathsf{1}\rangle\mathsf{1}+\tfrac{1}{2}\langle\mathsf{y},\mathsf{s}\rangle\mathsf{s}.$$

where the factor $\frac{1}{2}=\langle\mathsf{1},\mathsf{1}\rangle^{-1}=\langle\mathsf{s},\mathsf{s}\rangle^{-1}$ takes into account that the basis vectors are not normalized. The condition of y being a multiple of s enforces $\langle\mathsf{y},\mathsf{1}\rangle=0$. Therefore the mass moment of the inhomogeneity y must vanish. Consequently, equations (11) are supplemented by the following *solvability conditions*.

$$\left.\begin{aligned}
\langle D\mathsf{f}^{(0)},\mathsf{1}\rangle &= 0\\
\langle D\mathsf{f}^{(1)},\mathsf{1}\rangle &= -\tfrac{1}{2}\langle D^2\mathsf{f}^{(0)},\mathsf{1}\rangle\\
\langle D\mathsf{f}^{(2)},\mathsf{1}\rangle &= -\tfrac{1}{2}\langle D^2\mathsf{f}^{(1)},\mathsf{1}\rangle-\tfrac{1}{6}\langle D^3\mathsf{f}^{(0)},\mathsf{1}\rangle\\
\langle D\mathsf{f}^{(3)},\mathsf{1}\rangle &= -\tfrac{1}{2}\langle D^2\mathsf{f}^{(2)},\mathsf{1}\rangle-\tfrac{1}{6}\langle D^3\mathsf{f}^{(1)},\mathsf{1}\rangle-\tfrac{1}{24}\langle D^4\mathsf{f}^{(0)},\mathsf{1}\rangle
\end{aligned}\right\} \tag{13}$$

In the forthcoming paragraphs we extract from these equations:

- explicit formulas representing the asymptotic order functions in terms of their mass moments,
- evolution equations determining the mass moments.

Before we begin with this program we need to know the nullspace of $I-E$, which is given by the range of E, i.e.:

$$\operatorname{kernel}(I-E)=\operatorname{span}\left\{\tfrac{1}{2}\begin{pmatrix}1-a\\1+a\end{pmatrix}\right\}=\operatorname{span}\{\tfrac{1}{2}(1+a\mathsf{s})\}. \tag{14}$$

[6]The column vectors of $I-E$ in (12) are multiples of s, more precisely the left column vector is $(1+a)\mathsf{s}$, the right one $(-1+a)\mathsf{s}$.

Note, that the factor $\frac{1}{2}$ serves only to normalize the mass moment.

It shall be emphasized that we have not yet said anything, so far, about the existence of the prediction function. All we do is to derive necessary conditions, that must be fulfilled by a sufficiently smooth prediction function and its asymptotic order functions in order to generate a residual of the desired magnitude. However, as soon as we find functions complying with the obtained conditions, we can infer the existence of the prediction function.

Discussion of the 0^{th} order equation: representation of $\mathsf{f}^{(0)}$

Equation (11_0) implies that $\mathsf{f}^{(0)}(t,x)$ must belong to the kernel of $I-E$ independently of its arguments t,x. According to equation (14) $\mathsf{f}^{(0)}(t,x)$ should be a multiple of $\frac{1}{2}(\mathsf{1}+a\mathsf{s})$. The factor of proportionality, abbreviated by $u^{(0)}$, may vary with t,x like $\mathsf{f}^{(0)}$ itself and must be considered as a scalar function. So we get:

$$\boxed{\mathsf{f}^{(0)} = \tfrac{1}{2}(\mathsf{1}+a\mathsf{s})u^{(0)}} \tag{15}$$

At present, $u^{(0)}$ appears to be completely arbitrary. In the next paragraph we will see, that the solvability condition for equation (11_1) imposes the necessary constraints on $u^{(0)}$ to fix it. However, taking the scalar product[7] with $\mathsf{1}$ we recognize already now that $u^{(0)}$ plays the role of the mass moment pertaining to $\mathsf{f}^{(0)}$.

Discussion of the 1^{st} solvability condition: evolution of $u^{(0)}$

Writing down equation (13_0) being the solvability condition for (11_1), yields in detail:

$$\begin{aligned} 0 &= \langle D\mathsf{f}^{(0)}, \mathsf{1}\rangle = \tfrac{1}{2}\big\langle \big(\partial_t + \mathsf{s}\partial_x\big)\big(\mathsf{1}+a\mathsf{s}\big),\ \mathsf{1}\big\rangle u^{(0)} \\ &= \tfrac{1}{2}\big\langle \partial_t + \mathsf{s}(a\partial_t + \partial_x) + a\partial_x,\ \mathsf{1}\big\rangle u^{(0)} \\ &= \partial_t u^{(0)} + a\partial_x u^{(0)}\,, \end{aligned}$$

This shows, that $u^{(0)}$ must be a solution of the advection equation:

$$\boxed{\partial_t u^{(0)} + a\partial_x u^{(0)} = 0} \tag{16}$$

Discussion of the 1^{st} order equation: representation of $\mathsf{f}^{(1)}$

From linear algebra it is well known, that the general solution of an inhomogeneous, linear equation like (11_1) is composed of a specific solution plus an arbitrary solution of the homogeneous equation. In complete analogy to (11_0), the solution of the homogeneous equation $(I-E)\mathsf{f}^{(1)} = 0$ is given by $\frac{1}{2}(\mathsf{1}+a\mathsf{s})u^{(1)}$, where – similarly to $u^{(0)}$ above – $u^{(1)}$ is an unknown function to be determined later.

[7] Observe: $\langle \frac{1}{2}(\mathsf{1}+a\mathsf{s}), \mathsf{1}\rangle = 1$

How does a specific solution of the inhomogeneous equation $(I-E)\mathsf{x}=\mathsf{y}$ look like? From $E^2=E$ we conclude that $I-E$ is a projector too, because

$$(I-E)^2 \;=\; I^2-2E+E^2 \;=\; I-2E+E \;=\; I-E\,.$$

Hence, if $\mathsf{y}\in\text{image}(I-E)$ which entails $\mathsf{y}=(I-E)\mathsf{z}$ for some $\mathsf{z}\in\mathbb{R}^{\mathcal{S}}$, we conclude that

$$(I-E)\mathsf{y}=(I-E)^2\mathsf{z}=(I-E)\mathsf{z}=\mathsf{y},$$

which proves that y itself solves the equation $(I-E)\mathsf{x}=\mathsf{y}$ and is therefore a specific solution.

Applying this result we get the subsequent representation of $\mathsf{f}^{(1)}$

$$\mathsf{f}^{(1)}=\tfrac{1}{2}(1+a\mathsf{s})u^{(1)}-\tfrac{1}{\omega}D\mathsf{f}^{(0)},$$

which tacitly assumes the solvability condition $\langle D\mathsf{f}^{(0)},1\rangle=0$ or equivalently equation (16) to hold true. From this and $\langle\mathsf{s},1\rangle=0$ we deduce $\langle\mathsf{f}^{(1)},1\rangle=u^{(1)}$. Thus $u^{(1)}$ emerges as mass moment of $\mathsf{f}^{(1)}$.
In order to obtain a fully explicit expression we need to compute $D\mathsf{f}^{(0)}$.

$$\begin{aligned} D\mathsf{f}^{(0)} &= \tfrac{1}{2}(\partial_t+\mathsf{s}\partial_x)(1+a\mathsf{s})u^{(0)} \;=\; \tfrac{1}{2}\overbrace{(\partial_t+a\partial_x)u^{(0)}}^{=0}+\tfrac{1}{2}\mathsf{s}(a\partial_t+\partial_x)u^{(0)} \\ &= \tfrac{1}{2}(1-a^2)\mathsf{s}\partial_x u^{(0)} \end{aligned}$$

To get rid of the overbraced addend and to transmute the temporal derivative into a spatial one, we have applied equation (16) twice. With this preparation, we finally arrive at:

$$\boxed{\mathsf{f}^{(1)}=\tfrac{1}{2}(1+a\mathsf{s})u^{(1)}-\tfrac{1}{2\omega}(1-a^2)\mathsf{s}\partial_x u^{(0)}} \tag{17}$$

It is also easily checked by this formula, that $u^{(1)}$ corresponds to the mass moment of $\mathsf{f}^{(1)}$.

Extracting further orders: the general procedure

Before we enter the derivation of the evolution equations for $u^{(1)}$ and $u^{(2)}$, which might disguise the underlying thread, let us sketch how the computations proceed. We have seen by solving (11_0) and (11_1), that we are required to introduce a scalar function $u^{(\beta)}$ for each asymptotic order function. As a consequence of the solvability condition it turns out that $u^{(\beta)}$ has the meaning of the mass moment $\langle\mathsf{f}^{(\beta)},1\rangle$. Furthermore, $u^{(\beta)}$ is basically determined as a solution of an evolution equation that comes out from the solvability condition pertaining to the next order $\mathsf{f}^{(\beta+1)}$.

Using this knowledge we try to organize the computation of further asymptotic order functions more efficiently. So we introduce the $u^{(\beta)}$'s directly by setting

$u^{(\beta)} := \langle \mathsf{f}^{(\beta)}, \mathsf{1} \rangle$. Exchanging $E\mathsf{f}^{(\beta)}$ with $\mathsf{E}\big(u^{(\beta)}\big) =: \mathsf{E}^{(\beta)}$ we transform (11) into

$$\left.\begin{aligned}
\mathsf{f}^{(0)} &= \mathsf{E}^{(0)} \\
\mathsf{f}^{(1)} &= \mathsf{E}^{(1)} - \tfrac{1}{\omega} D\mathsf{f}^{(0)} \\
\mathsf{f}^{(2)} &= \mathsf{E}^{(2)} - \tfrac{1}{\omega} D\mathsf{f}^{(1)} - \tfrac{1}{2\omega} D^2\mathsf{f}^{(0)} \\
\mathsf{f}^{(3)} &= \mathsf{E}^{(3)} - \tfrac{1}{\omega} D\mathsf{f}^{(2)} - \tfrac{1}{2\omega} D^2\mathsf{f}^{(1)} - \tfrac{1}{6\omega} D^3\mathsf{f}^{(0)} \\
\mathsf{f}^{(4)} &= \mathsf{E}^{(4)} - \tfrac{1}{\omega} D\mathsf{f}^{(3)} - \tfrac{1}{2\omega} D^2\mathsf{f}^{(2)} - \tfrac{1}{6\omega} D^3\mathsf{f}^{(1)} - \tfrac{1}{24\omega} D^4\mathsf{f}^{(0)}
\end{aligned}\right\}. \tag{18}$$

In general we obtain

$$\mathsf{f}^{(\beta)} = \mathsf{E}^{(\beta)} - \tfrac{1}{\omega 1!} D\mathsf{f}^{(\beta-1)} - \ldots - \tfrac{1}{\omega \beta!} D^\beta \mathsf{f}^{(0)}. \tag{19}$$

This provides a recursive representation of the asymptotic order functions. After substituting β by β+1 and taking the scalar product with $\mathsf{1}$ we recover the solvability condition for $\mathsf{f}^{(\beta+1)}$

$$\langle D\mathsf{f}^{(\beta)}, \mathsf{1} \rangle = -\tfrac{1}{2} \langle D^2\mathsf{f}^{(\beta-1)}, \mathsf{1} \rangle - \ldots - \tfrac{1}{(\beta+1)!} \langle D^{\beta+1}\mathsf{f}^{(0)}, \mathsf{1} \rangle, \tag{20}$$

where we have additionally used the identity $\langle \mathsf{E}^{(\gamma)}, \mathsf{1} \rangle = u^{(\gamma)} = \langle \mathsf{f}^{(\gamma)}, \mathsf{1} \rangle$.
This equation is the point of departure for deriving the evolution equation of $u^{(\beta)}$. The first step is to insert the recursive representation of $\mathsf{f}^{(\beta)}$ into (20). Shoveling all scalar products with exception of the equilibrium term on the right hand side we arrive at

$$\langle D\mathsf{E}^{(\beta)}, \mathsf{1} \rangle = c_{\beta-1} \langle D^2\mathsf{f}^{(\beta-1)}, \mathsf{1} \rangle + \ldots + c_0 \langle D^{\beta+1}\mathsf{f}^{(0)}, \mathsf{1} \rangle,$$

with $c_{\beta-1}, ..., c_0$ denoting some coefficients. Independently of β, the left hand side becomes the differential operator $\partial_t + a\partial_x$ applied to $u^{(\beta)}$. So $u^{(\beta)}$ satisfies an advection equation that is driven by a source term depending on the mass moments $u^{(0)}, ..., u^{(\beta-1)}$ of the lower-order asymptotic order functions. To make the source more explicit, we employ recursively the representation formulas (counterparts of (19) for $\mathsf{f}^{(\beta-1)}, ..., \mathsf{f}^{(1)}$) and obtain eventually

$$\partial_t u^\beta + a\partial_x u^{(\beta)} = \tilde{c}_{\beta-1} \langle D^2\mathsf{E}^{(\beta-1)}, \mathsf{1} \rangle + \ldots + \tilde{c}_0 \langle D^{\beta+1}\mathsf{E}^{(0)}, \mathsf{1} \rangle$$

with some new constants $\tilde{c}_{\beta-1}, ..., \tilde{c}_0$. It only remains to expand the powers of D and to evaluate the scalar products. Then the source terms contain both spatial and temporal derivatives of the $u^{(\beta)}$'s. In order to eliminate the time derivatives, one successively resorts to the evolution equations for $u^{(0)}, \ldots, u^{(\beta-1)}$. Actually, this step[8] is the most tedious one of the whole computation. Concluding, we see that the computation can be performed quasi mechanically up to an arbitrary maximal order α.
Note, that we do not meet an equation for the mass moment of the highest order $u^{(\alpha)}$, because this would require to introduce a further asymptotic order function $\mathsf{f}^{(\alpha+1)}$. Without reducing the order of the residual we are free to choose $u^{(\alpha)}$. In accordance with the initial conditions (see next subsection) it can be set to 0.

[8] We remark that this step is not really necessary; furthermore it might be difficult to perform it in other situations, where the target equation is more complicated than the advection equation. The main reason for the replacement of temporal derivatives is to obtain finally expressions for the population functions that depend only on spatial derivatives. If we want to use these expressions to improve the initialization of the algorithm, it will be relatively easy to compute spatial derivatives of the initial data in contrast to time derivatives.

Evolution equation for $u^{(1)}$: Following the instruction from above we insert first (18_1) and then (18_0) into (13_1):

$$\begin{aligned}\langle D\mathsf{E}^{(1)},\mathsf{1}\rangle &= (\tfrac{1}{\omega}-\tfrac{1}{2})\langle D^2\mathsf{f}^{(0)},\mathsf{1}\rangle \\ &= (\tfrac{1}{\omega}-\tfrac{1}{2})\langle D^2\mathsf{E}^{(0)},\mathsf{1}\rangle\ .\end{aligned}$$

Next, we evaluate $\langle D\mathsf{E}^{(1)},\mathsf{1}\rangle = \partial_t u^{(1)} + a\partial_x u^{(1)}$ and

$$\begin{aligned}\langle D^2\mathsf{E}^{(0)},\mathsf{1}\rangle &= \tfrac{1}{2}\Big\langle \big(\partial_t^2 + 2\mathsf{s}\partial_t\partial_x + \partial_x^2\big)(\mathsf{1}+a\mathsf{s}),\ \mathsf{1}\Big\rangle\, u^{(0)} \\ &= \big(\partial_t^2+\partial_x^2+2a\partial_t\partial_x\big)u^{(0)} \ =\ (1-a^2)\partial_x^2 u^{(0)},\end{aligned}$$

where we have employed repeatedly (16) $\partial_t u^{(0)} = -a\partial_x u^{(0)}$ to eliminate the time derivatives. Combining the results produces the evolution equation for $u^{(1)}$.

$$\boxed{\partial_t u^{(1)} + a\partial_x u^{(1)} = (\tfrac{1}{\omega}-\tfrac{1}{2})(1-a^2)\partial_x^2 u^{(0)}} \tag{21}$$

Evolution equation for $u^{(2)}$: Once again we repeat the procedure. Plugging first (18_2) into (13_2) leads to

$$\langle D\mathsf{E}^{(2)},\mathsf{1}\rangle = \big(\tfrac{1}{\omega}-\tfrac{1}{2}\big)\langle D^2\mathsf{f}^{(1)},\mathsf{1}\rangle + \big(\tfrac{1}{2\omega}-\tfrac{1}{6}\big)\langle D^3\mathsf{f}^{(0)},\mathsf{1}\rangle\ .$$

Insertion of (18_1) for $\mathsf{f}^{(1)}$ and (18_2) for $\mathsf{f}^{(2)}$ gives

$$\langle D\mathsf{E}^{(2)},\mathsf{1}\rangle = \big(\tfrac{1}{\omega}-\tfrac{1}{2}\big)\langle D^2\mathsf{E}^{(1)},\mathsf{1}\rangle - \big(\tfrac{1}{\omega^2}-\tfrac{1}{\omega}+\tfrac{1}{6}\big)\langle D^3\mathsf{E}^{(0)},\mathsf{1}\rangle\ . \tag{22}$$

Since the left hand side ends up in the advection operator applied to $u^{(2)}$, it remains to care about the two addends of the right hand side. In order to eliminate finally all time derivatives, we express first $\partial_t^2 u^{(1)}$ by space derivatives of $u^{(1)}$ and $u^{(0)}$. For this we employ the evolution equations (21) and (16):

$$\begin{aligned}\partial_t^2 u^{(1)} &= -a\partial_x\partial_t u^{(1)} + (\tfrac{1}{\omega}-\tfrac{1}{2})(1-a^2)\partial_x^2\partial_t u^{(0)} \\ &= -a\partial_x\Big(-a\partial_x u^{(1)} + (\tfrac{1}{\omega}-\tfrac{1}{2})(1-a^2)\partial_x^2 u^{(0)}\Big) - (\tfrac{1}{\omega}-\tfrac{1}{2})a(1-a^2)\partial_x^3 u^{(0)} \\ &= a^2\partial_x^2 u^{(1)} - 2a(\tfrac{1}{\omega}-\tfrac{1}{2})(1-a^2)\partial_x^3 u^{(0)}.\end{aligned}$$

This preparation together with further substitutions using (21) and (16) then yields:

$$\begin{aligned}\langle D^2\mathsf{E}^{(1)},\mathsf{1}\rangle &= \tfrac{1}{2}\Big\langle(\partial_t^2+2\mathsf{s}\partial_t\partial_x+\partial_x^2)(\mathsf{1}+a\mathsf{s}),\mathsf{1}\Big\rangle u^{(1)} \ =\ \big(\partial_t^2+2a\partial_t\partial_x+\partial_x^2\big)u^{(1)} \\ &= a^2\partial_x^2 u^{(1)} - 2a(\tfrac{1}{\omega}-\tfrac{1}{2})(1-a^2)\partial_x^3 u^{(0)} \\ &\quad + \partial_x^2 u^{(1)} + 2a\partial_x\Big(-a\partial_x u^{(1)} + (\tfrac{1}{\omega}-\tfrac{1}{2})\partial_x^2 u^{(0)}\Big) \\ &= (1-a^2)\partial_x^2 u^{(1)}\end{aligned}$$

For the second addend we get; utilizing (16) again,

$$\begin{aligned}\langle D^3\mathsf{E}^{(0)},\mathsf{1}\rangle &= \tfrac{1}{2}\Big\langle\big(\partial_t^3+3\mathsf{s}\partial_t\partial_x^2+3\partial_t\partial_x^2+\mathsf{s}\partial_x^3\big)\big(\mathsf{1}+a\mathsf{s}\big),\ \mathsf{1}\Big\rangle u^{(0)} \\ &= \Big(\partial_t^3+3a\partial_t^2\partial_x+3\partial_t\partial_x^2+a\partial_x^3\Big)u^{(0)} \ =\ \Big(-a^3+3a^3-3a+a\Big)\partial_x^3 u^{(0)} \\ &= -2a(1-a^2)\partial_x^3 u^{(0)}.\end{aligned}$$

Combining these results with (22) eventually produces the evolution equation for $u^{(2)}$.

$$\boxed{\boldsymbol{\partial_t u^{(2)} + a\partial_x u^{(2)}} = (\tfrac{1}{\omega}-\tfrac{1}{2})(1-a^2)\boldsymbol{\partial_x^2 u^{(1)}} + 2a(\tfrac{1}{\omega^2}-\tfrac{1}{\omega}+\tfrac{1}{6})(1-a^2)\boldsymbol{\partial_x^3 u^{(0)}}} \tag{23}$$

Explicit representation of $\mathsf{f}^{(2)}$: In order to provide explicit expressions[9] for the asymptotic order functions we must go through the recursion as given by (18) and (19).
For $\mathsf{f}^{(2)}$ we start with the preliminary calculations to get $D\mathsf{f}^{(1)}$ and $D^2\mathsf{f}^{(2)}$:

$$D\mathsf{f}^{(1)} = \tfrac{1}{2}(1+a\mathsf{s})(\partial_t + \mathsf{s}\partial_x)u^{(1)} - \tfrac{1}{2\omega}(1-a^2)\mathsf{s}(\partial_t + \mathsf{s}\partial_x)\partial_x u^{(0)}$$

Eliminating the temporal derivatives by reverting to (16) and (21) we continue:

$$\begin{aligned} D\mathsf{f}^{(1)} &= \tfrac{1}{2}(1+a\mathsf{s})\Big(-a\partial_x u^{(1)} + (\tfrac{1}{\omega}-\tfrac{1}{2})(1-a^2)\partial_x^2 u^{(0)}\Big) + \tfrac{1}{2}(1+a\mathsf{s})\mathsf{s}\partial_x u^{(1)} \\ &\quad - \tfrac{1}{2\omega}(1-a^2)\mathsf{s}(-a\partial_x + \mathsf{s}\partial_x)\partial_x u^{(0)} \\ &= \tfrac{1}{2}(1-a^2)\mathsf{s}\partial_x u^{(1)} + \tfrac{1}{2}(1-a^2)\Big((\tfrac{1}{\omega}-\tfrac{1}{2})(1+a\mathsf{s}) - \tfrac{1}{\omega}(1-a\mathsf{s})\Big)\partial_x^2 u^{(0)} \\ &= \tfrac{1}{2}(1-a^2)\mathsf{s}\partial_x u^{(1)} + \tfrac{1}{2}(1-a^2)\Big(\tfrac{2}{\omega}a\mathsf{s} - \tfrac{1}{2}a\mathsf{s} - \tfrac{1}{2}\Big)\partial_x^2 u^{(0)} \end{aligned}$$

Likewise we obtain:

$$\begin{aligned} D^2\mathsf{f}^{(0)} &= \tfrac{1}{2}(1+a\mathsf{s})(\partial_t^2 + 2\mathsf{s}\partial_t\partial_x + \partial_x^2)u^{(0)} = \tfrac{1}{2}(1+a\mathsf{s})(a^2\partial_x^2 - 2a\mathsf{s}\partial_x^2 + \partial_x^2)u^{(0)} \\ &= \tfrac{1}{2}(1-a^2+a^3\mathsf{s}-a\mathsf{s})\partial_x^2 u^{(0)} = \tfrac{1}{2}(1-a^2)(1-a\mathsf{s})\partial_x^2 u^{(0)} \end{aligned}$$

Plugging these expressions into (18_2) yields

$$\begin{aligned} \mathsf{f}^{(2)} &= \mathsf{E}^{(2)} - \tfrac{1}{\omega}D\mathsf{f}^{(1)} - \tfrac{1}{2\omega}D^2\mathsf{f}^{(0)} \\ &= \tfrac{1}{2}(1+a\mathsf{s})u^{(2)} - \tfrac{1}{2\omega}(1-a^2)\mathsf{s}\partial_x u^{(1)} \\ &\quad - \tfrac{1}{2\omega}(1-a^2)\Big(\tfrac{2}{\omega}a\mathsf{s} - \tfrac{1}{2}a\mathsf{s} - \tfrac{1}{2}\Big)\partial_x^2 u^{(0)} - \tfrac{1}{4\omega}(1-a^2)(1-a\mathsf{s})\partial_x^2 u^{(0)} \end{aligned}$$

and finally:

$$\boxed{\mathsf{f}^{(2)} = \tfrac{1}{2}(1+a\mathsf{s})u^{(2)} - \tfrac{1}{2\omega}(1-a^2)\mathsf{s}\partial_x u^{(1)} - \tfrac{1}{2\omega}(\tfrac{1}{\omega}-\tfrac{1}{2})(1-a^2)a\mathsf{s}\partial_x^2 u^{(0)}} \tag{24}$$

3.2 Analysis of initial conditions

With the considerations above, we have come quite close to a thorough understanding of the lattice Boltzmann solution. Starting out with an asymptotic expansion $\mathsf{F}(t,x) \approx \mathsf{f}^{(0)}(t,x) + h\mathsf{f}^{(1)}(t,x) + h^2\mathsf{f}^{(2)}(t,x) + \ldots$, we derived the precise form of the leading order coefficients

$$\left.\begin{aligned} \mathsf{f}^{(0)} &= \tfrac{1}{2}(1+a\mathsf{s})u^{(0)} \\ \mathsf{f}^{(1)} &= \tfrac{1}{2}(1+a\mathsf{s})u^{(1)} - \tfrac{1}{2\omega}(1-a^2)\mathsf{s}\partial_x u^{(0)} \\ \mathsf{f}^{(2)} &= \tfrac{1}{2}(1+a\mathsf{s})u^{(2)} - \tfrac{1}{2\omega}(1-a^2)\mathsf{s}\partial_x u^{(1)} - \tfrac{1}{2\omega}(\tfrac{1}{\omega}-\tfrac{1}{2})(1-a^2)a\mathsf{s}\partial_x^2 u^{(0)} \end{aligned}\right\} \tag{25}$$

by exploiting the lattice Boltzmann update rule (4). However, the full lattice Boltzmann algorithm consists of (4) *and* the initialization condition (5)

$$\mathsf{F}(0,x) = \mathsf{E}(v_0(x)). \tag{26}$$

In order to ensure that our prediction function satisfies *all* the constraints imposed on the numerical solution as accurately as possible, we use (26) in exactly the same

[9] containing only (spatial) derivatives of the mass moments of equal and lower order

way as the update rule: we replace F in (26) by $\mathsf{f}^{[\alpha]}$ and compare h-coefficients. Due to the simplicity of the condition, we quickly find

$$\left.\begin{aligned} h^0: &\quad \mathsf{f}^{(0)}(0,x) = \tfrac{1}{2}(1+a\mathsf{s})v_0(x) \\ h^1: &\quad \mathsf{f}^{(1)}(0,x) = 0 \\ h^2: &\quad \mathsf{f}^{(2)}(0,x) = 0 \end{aligned}\right\} \tag{27}$$

Comparing (25_0) and (27_0), we see that the initialization constraint forces the initial condition $u^{(0)}(0,x) = v_0(x)$ for the leading order mass moment. In view of the fact that $u^{(0)}$ also satisfies (16), we conclude that $u^{(0)}$ and thus also $\mathsf{f}^{(0)}$ is now *completely* determined.
In the next order, we similarly find $u^{(1)}(0,x) = 0$ but also $\partial_x u^{(0)}(0,x) = 0$. The latter condition is clearly violated if the function v_0 is not constant because $u^{(0)}(0,x) = v_0(x)$ as a consequence of the previous consideration. In other words, for the lattice Boltzmann algorithm with initialization (26), our prediction function can only describe the numerical solution if v_0 is restricted to the boring case of constant functions. The reason for this behavior can be understood as follows: even if we set $u^{(1)}(0,x) = 0$, the evolution equation requires $\mathsf{f}^{(1)}(t,x) = -\frac{1}{2\omega}(1-a^2)\mathsf{s}\partial_x u^{(0)}(t,x)$ for all $(t,x) \in [0,T]\times\mathbb{R}$ whereas the initialization forces $\mathsf{f}^{(1)}(0,x) = 0$. These two conditions amount to a discontinuity of $\mathsf{f}^{(1)}$ at $t = 0$ unless v_0 is constant. In particular, a *smooth* prediction function as used in the expansion of the update rule, is incapable of describing this situation properly. Since smoothness has been an important ingredient in the derivation (Taylor's theorem), we conclude that our prediction function may properly describe the leading order h-dependence of the numerical solution but fails to describe the first order contribution.
Practically, we can observe the anticipated non-smoothness in first order as a consequence of initialization (26). An example is provided by figure 3.2.

As a remedy, we propose a modified initialization rule which avoids non-smoothness in the leading orders. We set[10]

$$\mathsf{F}(0,x) = \mathsf{E}(v_0(x)) - h\tfrac{1}{2\omega}(1-a^2)\mathsf{s}\partial_x v_0(x) - h^2\tfrac{1}{2\omega}(\tfrac{1}{\omega}-\tfrac{1}{2})(1-a^2)a\mathsf{s}\partial_x^2 v_0(x). \tag{28}$$

Analyzing the lattice Boltzmann algorithm with this initialization rule, we find

$$\left.\begin{aligned} h^0: &\quad \mathsf{f}^{(0)}(0,x) = \tfrac{1}{2}(1+a\mathsf{s})v_0(x) \\ h^1: &\quad \mathsf{f}^{(1)}(0,x) = -\tfrac{1}{2\omega}(1-a^2)\mathsf{s}\partial_x v_0(x) \\ h^2: &\quad \mathsf{f}^{(2)}(0,x) = -\tfrac{1}{2\omega}(\tfrac{1}{\omega}-\tfrac{1}{2})(1-a^2)a\mathsf{s}\partial_x^2 v_0(x) \end{aligned}\right\} \tag{29}$$

which is compatible with (25) if $u^{(0)}(0,x) = v_0(x)$ and $u^{(1)}(0,x) = u^{(2)}(0,x) = 0$.

[10] This idea can be generalized by setting $\mathsf{F}(0,x) = \mathsf{f}^{[\alpha]}(0,x)$ where all mass moments $u^{(\beta)}$ with $1 \le \beta \le \alpha$ are assumed to vanish initially and $u^{(0)}(0,x)$ is assumed to be $v_0(x)$. In this case, the initial condition only depends on v_0 and its derivatives. By construction, the initialization is compatible with the prediction $f^{[\alpha]}$ so that non-smoothness may only appear in order $\alpha+1$. From a practical point of view, the initial condition enforces $\langle \mathsf{F}(0,x), 1\rangle = v_0(x)$ so that v_0 has the interpretation as initial value for the mass moment of F.

In summary, our prediction function $\mathsf{f}^{[2]}$ satisfies the *full* lattice Boltzmann algorithm quite accurately, provided the asymptotic order functions are based on the mass moments satisfying the subsequent initial value problems (30), (31) and (32). For clarity we define the abbreviations:

$$\mu := (\tfrac{1}{\omega} - \tfrac{1}{2})(1 - a^2), \qquad \lambda := 2a(\tfrac{1}{\omega^2} - \tfrac{1}{\omega} + \tfrac{1}{6})(1 - a^2).$$

IVP for $u^{(0)}$:

$$\boxed{\begin{aligned} &\partial_t u^{(0)} + a\partial_x u^{(0)} = 0 \\ &u^{(0)}(0,x) = v_0(x) \end{aligned}} \tag{30}$$

IVP for $u^{(1)}$:

$$\boxed{\begin{aligned} &\partial_t u^{(1)} + a\partial_x u^{(1)} = \mu\partial_x^2 u^{(0)} \\ &u^{(1)}(0,x) = 0 \end{aligned}} \tag{31}$$

IVP for $u^{(2)}$:

$$\boxed{\begin{aligned} &\partial_t u^{(2)} + a\partial_x u^{(2)} = \mu\partial_x^2 u^{(1)} + \lambda\partial_x^3 u^{(0)} \\ &u^{(2)}(0,x) = 0 \end{aligned}} \tag{32}$$

We remark that $u^{(0)}$, $u^{(1)}$, $u^{(2)}$ are automatically 1-periodic if v_0 has this property. Furthermore these equations determine $u^{(0)}$, $u^{(1)}$ and $u^{(2)}$ unambiguously.

3.3 Consistency

We have seen that the prediction function $\mathsf{f}^{[2]}$ approximately satisfies the lattice Boltzmann algorithm (4) with initialization (28) if the asymptotic order functions and their mass moments are chosen according to (25) and (30), (31), (32). We can formally[11] conclude that $\mathsf{f}^{[2]}$ captures the h-behavior of F up to the expanded order, i.e. $\mathsf{F}(t,x) - \mathsf{f}^{[2]}(t,x) = \mathrm{O}(h^3)$. Summing over the components, we find for the mass moment at every grid point (t,x)

$$U(t,x) = u^{(0)}(t,x) + hu^{(1)}(t,x) + h^2u^{(2)}(t,x) + \mathrm{O}(h^3). \tag{33}$$

In particular, U coincides with the solution $u^{(0)}$ of (30) up to an error which is at least proportional to h. In this sense, our lattice Boltzmann algorithm is *consistent* to the advection equation (30). The order of consistency can also be deduced from (33). If $\omega \neq 2$ and $a^2 \neq 1$ and hence $\mu \neq 0$, equation (31) for $u^{(1)}$ involves a non-zero source term (unless v_0 is constant which would imply $\partial_x^2 u^{(0)} = 0$). Thus $u^{(1)}$ will be different from zero and the coincidence of U and $u^{(0)}$ is of first order

$$U(t,x) - u^{(0)}(t,x) = hu^{(1)}(t,x) + \mathrm{O}(h^2).$$

[11] The conclusion can be rigorously justified provided the lattice Boltzmann evolution operator can be shown to be *stable* which essentially requires all powers of the evolution matrix to be uniformly bounded in a suitable norm.

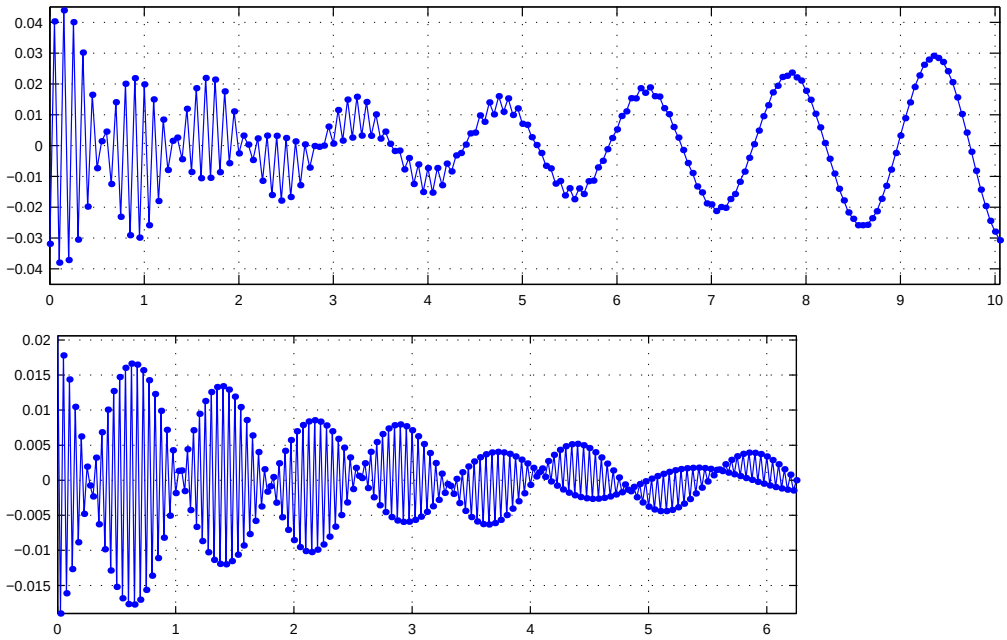

Figure 1:
The curves represent the quantity $\mathsf{F}_1(t,x) - \mathsf{f}_1^{[2]}(t,x)$ versus the time t in a fixed, single grid point x over 200 iterations on a mesh with 20 nodes with $\omega = 1.97$. In the upper graph the lattice Boltzmann algorithm has been initialized using the equilibrium with $v_0(x) = \cos(2\pi x)$. The lower curve refers to an improved, consistent initialization by means of the regular expansion, i.e. $\mathsf{F}(0,\cdot) = \mathsf{f}^{[2]}(0,\cdot)$. The deviation between F and $\mathsf{f}^{[2]}$ starts with 0 and increases quite slowly in time. Furthermore we observe a smoothly oscillating behavior which is explained by the advection of the cosine ($a = 0.66$). In contrast, the upper curve seems to be a superposition of the lower one with a strongly oscillating (from iteration to iteration) initial deviation due to the inconsistent initialization violating the smoothness assumptions concerning the asymptotic order functions and their mass moments. However, the initial layer ebbs down after around 100 iterations.

We say that the algorithm is *first order consistent* to (30) in that case. If, however, $\omega = 2$ or $a^2 = 1$, the source term in (31) vanishes and since $u^{(1)}(0,x) = 0$, the solution $u^{(1)}(t,x)$ turns out to be zero everywhere. In this case,

$$U(t,x) - u^{(0)}(t,x) = h^2 u^{(2)}(t,x) + \mathrm{O}(h^3)$$

where $u^{(2)}$ is non-zero for non-trivial $u^{(0)}$ and $a^2 \notin \{0,1\}$ (note that for $\omega = 2$, the factor $\lambda = 2a(1-a^2)(\frac{1}{\omega^2} - \frac{1}{\omega} + \frac{1}{6})$ equals $-\frac{1}{6}a(1-a^2)$). Hence, the lattice Boltzmann method is a second order accurate method for (30) in the case $\omega = 2$.
For $a^2 = 1$, the $u^{(2)}$-equation has zero source and zero initial value so that $u^{(2)} = 0$ in that case. Then, the algorithm is at least third order accurate[12].
We conclude that the proposed lattice Boltzmann algorithm gives rise to approximate solutions of the advection problem (30) with first, second, or higher order of consistency, depending on the chosen parameters.
In exactly the same way, other lattice Boltzmann algorithms [2, 3, 5, 6, 7, 1] or, more generally, any finite difference scheme [4] can be analyzed.

3.4 Explicit computation of the mass moments

Due to the simplicity of the scenario considered here, we are able to solve the equations for the mass moments analytically. This step is actually not necessary for the consistency analysis which can be carried out just based on the homogeneous or non-homogeneous structure of the equations as demonstrated above. However, the explicit solution reveals some interesting structure which naturally leads to a multiscale analysis of the algorithm. The equations (30), (31), and (32) are advection problems which can be solved with the method of characteristics.

To explain the idea, let us consider a problem of the general form

$$\partial_t w + a\partial_x w = b, \qquad w(0,x) = w_0(x). \tag{34}$$

The equation states that the directional derivative of w along the constant vector $(1,a)$ in (t,x) space is given by the function b. Considering a characteristic line $\sigma \mapsto Y(\sigma)$ starting in the point $(0,x_0)$ with direction vector $(1,a)$, i.e.

$$\dot{Y}(\sigma) = (1,a), \quad Y(0) = (0,x_0) \qquad \Rightarrow \qquad Y(\sigma) = (\sigma, x_0 + \sigma a),$$

we know that the value $z(\sigma)$ of the solution to (34) evolves along the line according to the law

$$\dot{z}(\sigma) = b(Y(\sigma)), \qquad z(0) = w_0(x_0).$$

In particular, the solution w at a given point (t,x) is obtained by determining x_0 and σ such that $Y(\sigma) = (t,x)$ and setting $w(t,x) = z(\sigma)$. Specifically, we have $\sigma = t$ and $x_0 = x - at$, so that

$$w(t,x) = z(t), \qquad \dot{z}(\sigma) = b(\sigma, x - (t-\sigma)a), \qquad z(0) = w_0(x - at).$$

Applying this methodology to (30), we have to deal with the simple source $b^{(0)}(t,x) = 0$ so that z turns out to be constant along the characteristic line, i.e. $z(\sigma) = w_0(x - at)$ for all σ. Hence:

$$\boxed{u^{(0)}(t,x) = v_0(x - at)} \tag{35}$$

[12] One can show that for $a^2 = 1$, the lattice Boltzmann algorithm even reproduces the *exact* solution of (30) at the grid points.

Using this result, we can compute the right hand side of (31)

$$b^{(1)}(t,x) = \mu v_0''(x-at), \qquad \mu = (\tfrac{1}{\omega} - \tfrac{1}{2})(1-a^2).$$

Along the characteristic line, we have

$$b^{(1)}(\sigma, x-(t-\sigma)a)) = \mu v_0''(x-(t-\sigma)a - a\sigma) = \mu v_0''(x-at)$$

which is independent of σ. Hence, the function value z grows with constant rate $v_0''(x-at)$ along the characteristic, starting with $u^{(1)}(0, x-at) = 0$ so that:

$$\boxed{u^{(1)}(t,x) = \mu t v_0''(x-at)} \tag{36}$$

The source in (32) has the form

$$b^{(2)}(t,x) = \mu \partial_x^2 u^{(1)}(t,x) + \lambda \partial_x^3 u^{(0)}(t,x), \qquad \lambda = 2a(\tfrac{1}{\omega^2} - \tfrac{1}{\omega} + \tfrac{1}{6})(1-a^2).$$

Similarly to the previous case, the behavior is simple along the characteristics with the only difference, that the linear growth of $u^{(1)}$ is integrated to a quadratic behavior. More precisely,

$$b^{(2)}(\sigma, x-(t-\sigma)a)) = \mu^2 \sigma v_0''''(x-at) + \lambda v_0'''(x-at)$$

and thus:

$$\boxed{u^{(2)}(t,x) = \tfrac{1}{2}\mu^2 t^2 v_0''''(x-at) + \lambda t v_0'''(x-at)} \tag{37}$$

Using this explicit form, we can write

$$U(t,x) = v_0(y) + (ht)\mu v_0''(y) + \tfrac{1}{2}(ht)^2 \mu^2 v_0''''(y) + (h^2 t)\lambda v_0'''(y) + \mathrm{O}(h^3)\big|_{y=x-at}.$$

An important observation is that the expansion *breaks down* if t is chosen large. For example, if $t = 1/h$, the formerly first and second order terms obviously turn into zero order contributions and we may expect that higher order terms which we collected in $\mathrm{O}(h^3)$ also need to be considered since they may be of the form $(ht)^3$, $(ht)^4$, etc. In other words, the regular expansion fails to represent the leading order behavior for large t since it is non-uniform in the time variable (it contains so-called *secular*[13] terms). Hence, if we are interested in the long time behavior of our scheme, we have to choose a different asymptotic ansatz. Such an ansatz can be motivated by restructuring the expansion of U

$$U(t,x) = v_0(y) \; + \; \left[\mu v_0''(y) + h\lambda v_0'''(y)\right] ht \; + \; \tfrac{1}{2}\mu^2 v_0''''(y)\,(ht)^2 \; + \; \cdots\big|_{y=x-at} \; .$$

In this form U appears as some sort of truncated power series expansion in the variable (ht) where the coefficients itself are regularly expanded with respect to h and depend on t. Clearly, this truncation is reasonable if ht is small but fails for

[13] Derived from the Latin word *saeculum* = century. The term originates from celestial mechanics, more exactly from asymptotic expansions describing the motion of planets, and refers to long term perturbations. In our context we call terms in an asymptotic expansion secular (with respect to the time variable) if they are not uniformly bounded over $\mathbb{R}^+$ but only over compact intervals. However there is no strict definition.

$ht > 1$. The way out is to *avoid* expanding the distinct ht behavior with respect to h. Instead, the dependence of the numerical solution on the quantity ht should be resolved directly. This can be achieved with an ansatz of the form

$$U(t,x) = u^{(0)}(t,ht,x) + hu^{(1)}(t,ht,x) + h^2u^{(2)}(t,ht,x) + \dots$$

which is a so called two-scale expansion. An additional motivation for this approach can be drawn from direct observations of the numerical solution. This is explained in the following section.

4 Multiscale Expansion

4.1 A numerical experiment to detect different time scales

Consider the LB algorithm on two different spatial grids $\mathcal{G}_1 \subset \mathcal{G}_2$ with h_1 being a multiple of h_2. Both algorithms are supposed to be equally initialized by means of a smooth function v_0 representing the initial mass moment. Let $U_1(n)$ and $U_2(n)$ denote the mass moments on the coarse and fine grid after n iterations.
For a moment, we want to ignore the analysis done in section 3. Then it is not clear *a priori*, how U_1 and U_2 are related to each other. To be less sketchy we may ask, for which indices n_1, n_2 the mass moments $U_1(n_1)$ and $U_2(n_2)$ look especially similar.

We attempt to answer the question by an experiment. If the algorithm is initialized choosing a peak-like profile for v_0, one might discover[14] that the peaks almost coincide with each other if the iteration indices satisfy $n_1h_1 = n_2h_2$. More generally, we can say

$$U_1(n_1) \approx U_2(n_2) \qquad \text{whenever } n_1h_1 = n_2h_2. \tag{38}$$

Therefore it is reasonable to introduce a new quantity T_1 defined by $T_1(n_i, \mathcal{G}_i) := n_ih_i$ called *time*. Obviously, the evolution of the algorithm reveals a grid independent dynamics, if iterations on different grids are identified with respect to their time.
The strong resemblance (quasi-agreement) of the mass moments for $T_1(n_1, \mathcal{G}_1) = T_1(n_2, \mathcal{G}_2)$ is explained by the consistency analysis. This tells, that for $h \to 0$ the mass moments converge towards the solution of the advection equation (initialized by v_0), which, of course, does not know anything about the LB algorithm and thus displays a grid independent evolution.
If the two algorithms run over long periods with $T_1 \gg 1$, we realize that the peaks start to deform their shape (see figure 2). Although this phenomenon is predicted by the regular expansion (specifying the laeding error terms $u^{(1)}, u^{(2)}$) the forecast becomes totally wrong after a relatively short while. Furthermore we observe that the flattening of the peak is more distinct on the coarser grid $\mathcal{G}_1$ than on $\mathcal{G}_2$, in spite of comparing iterations corresponding to the same time. This insinuates that the deformation process takes place in a time scale different from that of the advection. In order to study the deformation alone without being "disturbed" by the advection it is possible to switch it off by setting $a = 0$. It turns out that the peaks

[14] The effect becomes the more evident the smaller h_1 and h_2 are chosen.

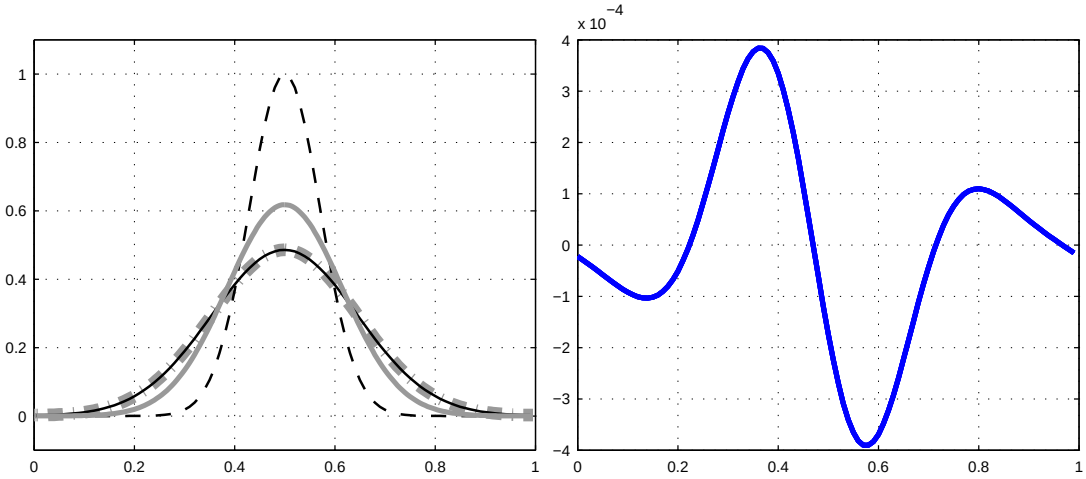

Figure 2:
Left: Advective(linear) versus diffusive(quadratic) time scale. Generally, the flattening of the mass moment increases with the number of iterations. Here we have set $\omega = 1.3$ and the advection velocity $a = 0.5$ has been chosen in such a way that the peak returns to its initial position at the center after 200(400) iterations on a grid with 100(200) nodes. So we can blind out the displacement by the advection avoiding to switch it off totally. The subsequent table indicates to which grid and to which iteration the lines (representing the mass moment) refer.

line	#grid nodes	#time steps
gray, dash-dotted	100 ($\mathcal{G}_1$)	400
gray, solid	200 ($\mathcal{G}_2$)	800
black solid	200 ($\mathcal{G}_2$)	1600

The fact that the black solid curve agrees with the gray dash-dotted curve suggests that the flattening occurs in the *quadratic time scale*. The black dashed peak corresponds to the initial condition. Right: Difference between the dash-dotted and the thin black solid line (projected onto the coarse grid).

undergo the same deformation on both grids, if the iteration indices fulfill the condition $n_1 h_1^2 = n_2 h_2^2$ (cf. figure 2). Similarly to T_1 we therefore define another time T_2 with $T_2(n, \mathcal{G}) := nh^2$, which elapses slower than T_1 provided $h < 1$. In order to distinguish both of the times we refer to T_1 as *linear time* and designate T_2 as *quadratic time*. Moreover we also speak of *time scales* in this context.

A special situation is observed for $\omega = 2$. Instead of a flattening, the deformation of the mass moment expresses itself by a distortion due to oscillations (cf. figure 3). It turns out, that these oscillations evolve (emerge and modify themselves) even slower than the quadratic time scale. This urges the conjecture that their evolution can be described by means of the cubic time scale $\big($introducing $T_3(n, \mathcal{G}) = nh^3\big)$, which is backed by figure 3.

Recapitulating we can say that the the evolution of our lattice Boltzmann algorithm appears as a superposition of several[15] processes. Each one is governed by a time scale of its own and can be interpreted as a grid independent process if regarded in this scale. In the next subsection we apply the technique of multiscale expansions to separate these processes from each other and to derive equations determining their evolution.

[15] Here we could also broach the issue of *initial layers* representing a typical example of superposed processes. Numerical initial layers are often triggered by crude initializations and evolve on a faster time scale than the dominant one, which is of interest for the user of the algorithm. Some initial layers evolve with respect to the *discrete time scale* ($T_0(n, \mathcal{G}) = n$).

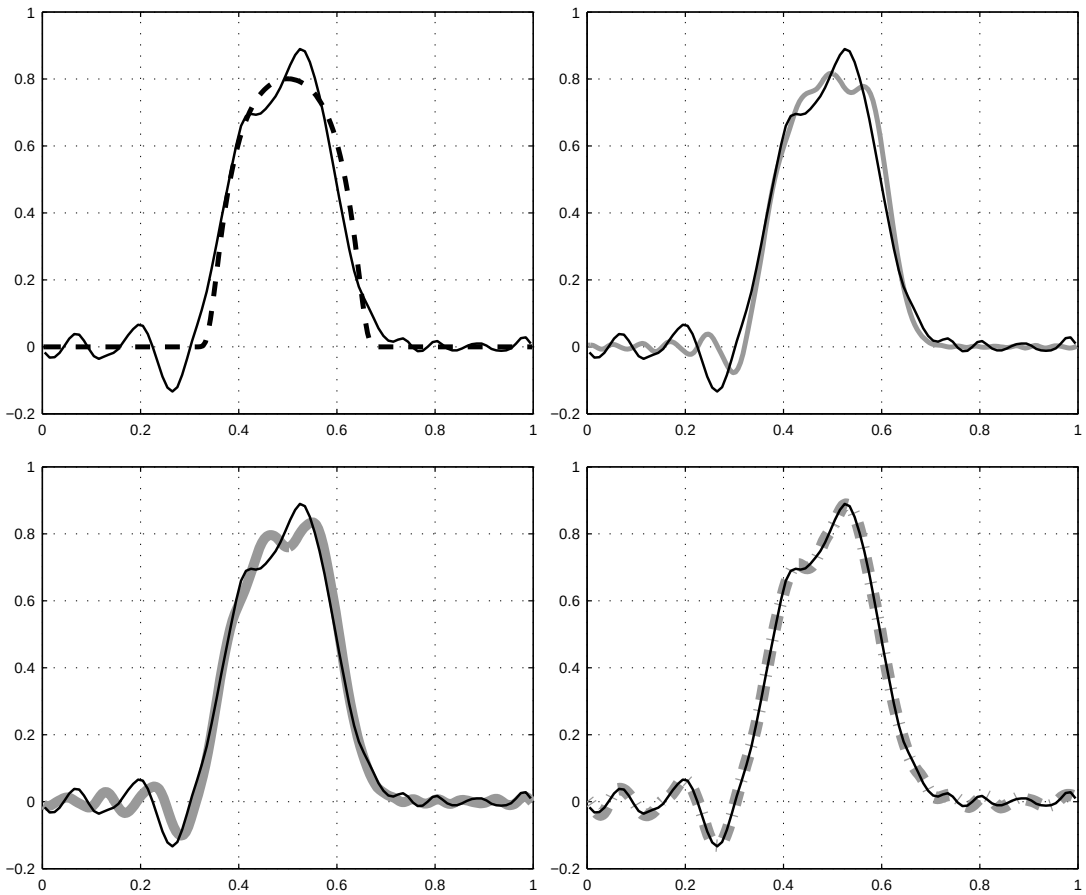

Figure 3:

Advective(linear) versus diffusive(quadratic) and dispersive(cubic) time scale: The plots display the mass moment on two different grids at different iterations (see table below). For clarity each diagram shows two curves only. The initial mass moment is given by the dashed line in the upper left subfigure. The flanks of this curve are quite steep near the transition point where the flat zone passes over to the peak. Although it seems to have kinks at the transition points, the function is everywhere arbitrarily smooth. As this feature provokes relatively strong oscillations it is well suited to highlight the effect. Observe that the two mass moments in the subfigure below at right match so well, that they appear virtually identical. As $3200 = 2^3 \cdot 200$, there are 8 times more iterations necessary to reach the same configuration of oscillations on a grid with half the spacing size. This prompts us to assume that the evolution of the oscillations becomes grid-independent if considered in the cubic time scale.

line	#grid nodes	#time steps
black solid	100	400
gray solid	200	800
gray solid (thick)	200	1600
gray dash-dotted	200	3200

Analogously to the example in figure 2 the advection velocity is set to $a = 0.5$, while we have selected the special value $\omega = 2$ for the relaxation frequency.

4.2 Additional quadratic time scale

The previous subsection gives rise to a modification of the ansatz for the prediction function. In order to capture both the advection in the linear time scale and the flattening deformation in the quadratic time scale we equip the new prediction function with two time arguments:

$$\mathsf{f}^{[\alpha]}(t_1,t_2,x) := \mathsf{f}^{(0)}(t_1,t_2,x) \;+\; h\mathsf{f}^{(1)}(t_1,t_2,x) \;+\; \ldots \;+\; h^\alpha \mathsf{f}^{(\alpha)}(t_1,t_2,x), \tag{39}$$

Inspired by the observations, we want to choose $\mathsf{f}^{[\alpha]}$ in such a way that we have

$$\mathsf{F}(t,x) \approx \mathsf{f}^{[\alpha]}(t,ht,x) \tag{40}$$

for $t = t_n = nh$ and $x = x_j = jh$ with $n \in \mathbb{N}_0$ and $j \in \mathbb{Z}$. In particular, $\mathsf{f}^{[\alpha]}$ shall satisfy the update rule (2) of the lattice Boltzmann algorithm with a small residual.

$$\mathsf{f}_k^{[\alpha]}(t+h,ht+h^2,x+s_kh) = \mathsf{f}_k^{[\alpha]}(t,ht,x) + \left[J\mathsf{f}^{[\alpha]}(t,ht,x)\right]_k + \mathrm{O}(h^{\alpha+1}) \tag{41}$$

We suppose that $\mathsf{f}^{[\alpha]}$ and its asymptotic order functions fulfill the same assumptions concerning the regularity, 1-periodicity etc. as in subsection 3.1. Next, we substitute (39) into (41). In order to find determining conditions for the $\mathsf{f}^{(\beta)}$'s we perform on the left hand side a Taylor expansion of each $\mathsf{f}^{(\beta)}$ around (t,ht,x). More precisely, the formal Taylor series

$$\left[\mathsf{f}_k^{(\beta)}(t+h,ht+h^2,x+s_kh)\right]_k = \sum_{\gamma\geq 0} \frac{1}{\gamma!}(hD+h^2\partial_{t_2})^\gamma\, \mathsf{f}^{(\beta)}(t,ht,x)$$

is truncated after the $(\alpha-\beta)^{\text{th}}$ order. Terms being of h-order greater than α (including the remainder terms of the Taylor expansion) are incorporated into the $\mathrm{O}(h^{\alpha+1})$-term. There is now some liberty to decide how the terms shall cancel each other. A reasonable way[16] is to equate those terms at the left and right hand side which carry the same power of h as prefactor. Then we obtain the following equations from the $0^{\text{th}}, 1^{\text{st}}, 2^{\text{nd}}$ and 3^{rd} order:

$$\left.\begin{aligned}
h^0 :&\quad \mathsf{f}^{(0)} &&= (I+J)\mathsf{f}^{(0)}\\
h^1 :&\quad \mathsf{f}^{(1)} + D\mathsf{f}^{(0)} &&= (I+J)\mathsf{f}^{(1)}\\
h^2 :&\quad \mathsf{f}^{(2)} + D\mathsf{f}^{(1)} + \tfrac{1}{2}D^2\mathsf{f}^{(0)} + \partial_{t_2}\mathsf{f}^{(0)} &&= (I+J)\mathsf{f}^{(2)}\\
h^3 :&\quad \mathsf{f}^{(3)} + D\mathsf{f}^{(2)} + \tfrac{1}{2}D^2\mathsf{f}^{(1)} + \tfrac{1}{6}D^3\mathsf{f}^{(0)} + \partial_{t_2}\mathsf{f}^{(1)} + D\partial_{t_2}\mathsf{f}^{(0)} &&= (I+J)\mathsf{f}^{(3)}
\end{aligned}\right\} \tag{42}$$

[16] We proceed as if we could perform the comparison of coefficients. But actually, the $\mathsf{f}^{(\beta)}(t,ht,x)$'s at the left hand side are not completely expanded with respect to h. Therefore the equality of terms containing the same power of h is not compellent if h is varied. Hence we are not lead automatically to equations that determine the asymptotic order functions as in the case of the regular expansion. Other settings are imaginable. This insinuates that multiscale expansions are not unique in contrast to regular expansions. To illustrate this by a trivial example consider the function $f(n) = nh+nh^2+n^2h^5$. Introducing the variables $t_1 = nh$ and $t_2 = nh^2$ there is an infinite multitude of possibilities. As the replacement of the third addend is not obvious we can express it using either t_1 or t_2 or both of them by writing it in the from $n^2h^5 = qn^2h^5 + (1-q)n^2h^5$ for some $q \in \mathbb{R}$. Hence we obtain the following parameterized family of representations

$$f_q(t_1,t_2) = (t_1+t_2) + hqt_2^2 + h^3(1-q)t_1^3,$$

all of them satisfying $f(n) = f_q(nh,nh^2)$.

Subtracting $\mathsf{f}^{(\beta)}$ on each side of (42_β) results in an equation for $\mathsf{f}^{(\beta)}$ with the system matrix $J = \omega(E - I)$. So the equations (42) correspond to (10). In particular we obtain the same equations in the 0^{th} and 1^{st} order; only the equations from the 2^{nd} order on are affected by the modified ansatz, producing additional inhomogeneities. As the structure of the equations stays unaltered, we can take over the results from subsection 3.1 tracking only the additional terms.

Introducing the mass moments $u^{(0)}, u^{(1)}, u^{(2)}$ and taking the scalar product of the equations in (42) with the vector $\mathsf{1}$ finally gives the subsequent equations[17]:

$$\left.\begin{aligned}
(42_1) \quad &\Rightarrow \quad \partial_{t_1} u^{(0)} + a\partial_x u^{(0)} = 0 \\
(42_2) \quad &\Rightarrow \quad \partial_{t_1} u^{(1)} + a\partial_x u^{(1)} = \mu\partial_x^2 u^{(0)} - \boldsymbol{\partial_{t_2} u^{(0)}} \\
(42_3) \quad &\Rightarrow \quad \partial_{t_1} u^{(2)} + a\partial_x u^{(2)} = \mu\boldsymbol{\partial_x^2 u^{(1)}} + \lambda\partial_x^3 u^{(0)} - \boldsymbol{\partial_{t_2} u^{(1)}}
\end{aligned}\right\} \tag{43}$$

In subsection 3.4 we have seen that the integration of the evolution equations for $u^{(1)}$ and $u^{(2)}$ lead to *secular* terms, that do not reflect the behavior of the algorithm on a long time scale. These terms are generated by the sources. A particular reason, why secular terms show up, is, that the sources are themselves solutions of (inhomogeneous) advection equations with equal advection velocity causing the unbounded factors t and t^2.
A view at (43_2) shows that we should encounter the same problem unless we require the right hand side of (43_2) to vanish. In fact, by this setting[18], we kill two birds with one stone: Firstly, we avoid the arising of secular terms. Secondly, we find a well known (homogeneous) diffusion equation, that determines the evolution of $u^{(0)}$ with respect to t_2.
Analogously we proceed with the next equation (43_3) which is decoupled into a homogeneous advection equation for $u^{(2)}$ and a diffusion equation for $u^{(1)}$. This time, the source term containing $u^{(0)}$ drives the diffusion equation for $u^{(1)}$ instead of the advection equation for $u^{(2)}$. We will see that this prevents the appearance of secular terms.

To summarize the reasoning, let us write down the initial value problems that determine $u^{(0)}$ and $u^{(1)}$, where the initial conditions result from the requirement $v_0(x) = \langle \mathsf{F}(0,x), \mathsf{1}\rangle = \langle \mathsf{f}^{[\alpha]}(0,0,x), \mathsf{1}\rangle$:

$$\boxed{\begin{aligned}
\partial_{t_1} u^{(0)}(t_1,t_2,x) \;+\; a\partial_x u^{(0)}(t_1,t_2,x) \;&=\; 0 \\
\partial_{t_2} u^{(0)}(t_1,t_2,x) \;-\; \mu\partial_x^2 u^{(0)}(t_1,t_2,x) \;&=\; 0 \\
u^{(0)}(0,0,x) &= v_0(x)
\end{aligned}} \tag{44}$$

[17] Observe that the scalar product $\langle D\partial_{t_2}\mathsf{f}^{(0)}, \mathsf{1}\rangle = \partial_{t_2}\langle D\mathsf{f}^{(0)}, \mathsf{1}\rangle = \partial_{t_2}\big(\underbrace{\partial_{t_1} u^{(0)} + a\partial_x u^{(0)}}_{=0}\big) = 0$ does not contribute.

[18] Notice that we only give a motivation and no strict justification for our approach, which has the appeal to break up a complicated, unconventional system into standard partial differential equations (similarly to separation of variables for Laplacian in spherical coordinates etc.). To reassure a reader being alarmed about this frivolity we recall that asymptotics often requires some ingenuity to select good ansatz. A rigorous proof is mostly based on a stability analysis and rarely reflects the idea, why a certain ansatz has been chosen. Furthermore it should be kept in mind that multiscale expansions need not be unique.

$$\boxed{\begin{array}{rcrcl} \partial_{t_1} u^{(1)}(t_1,t_2,x) & + & a\partial_x u^{(1)}(t_1,t_2,x) & = & 0 \\ \partial_{t_2} u^{(1)}(t_1,t_2,x) & - & \mu\partial_x^2 u^{(1)}(t_1,t_2,x) & = & \lambda\partial_x^3 u^{(0)}(t_1,t_2,x) \\ & & u^{(1)}(0,0,x) = 0 & & \end{array}} \tag{45}$$

A first hint locating the reason for the flattening deformation observed previously (cf. figure 2) is given by the occurrence of the diffusion equation (second equation in (44) and (45)). Indeed, the smoothing of sharp extrema and the leveling of steep slopes is the typical dynamics encoded in this equation and distinguishes it fundamentally from the advection equation. A necessary condition for the diffusion equation to display this behavior is the positivity of the *diffusivity coefficient* $\mu = (\frac{1}{\omega} - \frac{1}{2})(1 - a^2)$ determining how fast the smoothing process takes place. In case of $\mu < 0$ the smoothing behavior is reversed (ill-posedness of the backward diffusion equation) and the solution behaves in a 'bad' manner, what the lattice Boltzmann algorithm reflects by an instable comportment. In allusion to physical diffusion processes the (artificial) smoothing effect of numerical schemes is referred to as *numeric diffusion*[19].

For each mass moment we interprete the equation systems (44) and (45) as two initial value problems that are coupled via a common initial condition and the spatial variable x. The solution can be obtained consecutively starting with the diffusion equation.

In order to acquire some feeling, how possible solutions of (44) and (45) are constructed and look like, let us consider an example. Since we are primarily interested in 1-periodic solutions we choose a cosine[20] as initial mass moment:

$$v_0(0,0,x) = \cos(2\pi m x) \qquad m \in \mathbb{N}.$$

At first solving the diffusion equation yields:

$$u^{(0)}(0,t_2,x) = \exp\big(-4\pi^2 m^2 \mu t_2\big)\, \cos\big(2\pi m x\big)$$

Initializing the advection equation by $u^{(0)}(0,t_2,x)$, where t_2 is to be treated as a mere parameter, results in the final solution:

$$\boxed{u^{(0)}(t_1,t_2,x) = \exp\big(-4\pi^2 m^2 \mu t_2\big)\, \cos\big(2\pi m(x - a t_1)\big)} \tag{46}$$

The diffusion equation for $u^{(1)}$ is inhomogeneous. The source itself is a solution of a homogeneous diffusion equation with equal diffusivity μ. Therefore $u^{(1)}$ is just obtained by multiplying $\lambda\partial_x^3 u^{(0)}$ with t_2:

$$u^{(1)}(0,t_2,x) = 8\pi^3 m^3 \lambda \boldsymbol{t_2}\, \exp\big(-4\pi^2 m^2 \mu t_2\big)\, \sin\big(2\pi m x\big)$$

[19] Numeric diffusion may be regarded as an undesired and annoying property. However, in many situations it has a stabilizing side action.

[20] Actually, this example is of much importance, since $\cos(2\pi m x)$ represents the general Fourier mode. Thanks to the linearity of both equations the solution for an arbitrary 1-periodic initial function v_0 can be obtained by decomposing it into its Fourier modes. Solving the equations for each Fourier mode separately, the solution pertaining to the original initial value is recovered by superposition.

Substituting x by $x - at_1$

$$\boxed{u^{(1)}(t_1, t_2, x) = 8\pi^3 m^3 \lambda \, \mathbf{t}_2 \, \exp\big(-4\pi^2 m^2 \mu t_2\big) \, \sin\big(2\pi m(x - at_1)\big)} \qquad (47)$$

makes $u^{(1)}$ satisfy all three equations in (45).

Similar to (36), we notice a factor t_2 in the explicit representation of $u^{(1)}$. However, in opposition to the regular expansion, the factor t_2 is accompanied by the exponential function $\exp\big(-4\pi^2 m^2 \mu t_2\big)$ damping $u^{(1)}$ to zero while t_2 grows towards infinity, if the diffusion coefficient μ is positive. So, under this condition, $u^{(1)}$ is uniformly bounded, i.e. there are upper and lower bounds for all $t \geq 0$).

The situation in the first order is characteristic for higher orders, because the structure of the evolution equations

$$\begin{array}{rcrcl} \partial_{t_1} u^{(\beta)}(t_1, t_2, x) & + & a\partial_x u^{(\beta)}(t_1, t_2, x) & = & 0 \\ \partial_{t_2} u^{(\beta)}(t_1, t_2, x) & - & \mu\partial_x^2 u^{(\beta)}(t_1, t_2, x) & = & \text{inhomogeneity} \\ & & u^{(\beta)}(0, 0, x) = 0 & & \end{array}$$

is repeated for all $\beta \in \mathbb{N}$. The only difference is given by the inhomogeneities that become more complicated for higher orders. This entails particularly that t_2^β occurs as factor in the explicit formula for $u^{(\beta)}$. However, also higher powers of t_2 are tamed by the exponential function which decays more rapidly than any polynomial can increase. So $t_2^\beta \exp(-4\pi^2 m^2 \mu h t_2)$ is uniformly bounded for any β and vanishes at infinity ($t \uparrow \infty$). Therfore we are allowed to conclude that the two-scale expansion avoids secular terms.

The computations give rise to the hypothesis that the mass moment $U = \langle \mathsf{F}, \mathsf{1} \rangle$ admits the representation

$$U(t, x) = u^{(0)}(t, ht, x) + h u^{(1)}(t, ht, x) \; + \; \text{H.O.T}$$

where H.O.T. stands for 'higher order terms' and

$$\begin{aligned} &u^{(0)}(t, ht, x) + h u^{(1)}(t, ht, x) = \\ &\quad = \Big[\cos\big(2\pi m(x - at)\big) + h^2 t \, 8\pi^3 m^3 \lambda \sin\big(2\pi m(x - at)\big) \Big] \exp(-4\pi^2 m^2 \mu h t). \end{aligned}$$

Not that the factor h^2 in front of the sine comes from the first order and the substitution $t_2 = ht$. Under the assumption that the higher order terms are well-behaved, we infer:

- $u^{(0)}(t, ht, x)$ describes the behavior of $U(t, x)$ with 2^{nd} order accuracy in h on time intervals whose length is of magnitude O(1). This means that the maximal iteration index $n_{\max}$ satisfies the estimate $n_{\max} h < C$, where h denotes the grid spacing and C is a given constant.
- $u^{(0)}(t, ht, x)$ describes the behavior of U with 1^{st} order accuracy in h on 'long' time intervals whose length is of magnitude $\mathrm{O}(\frac{1}{h})$, i.e. the maximal iteration index complies with the condition $n_{\max} h^2 < C$.

In particular, our results for $u^{(0)}$ and $u^{(1)}$ in (46) and (47) foreshadow that U remains bounded independently of the number of iterations, if the algorithm is stable.

Indeed, all hypotheses are positively validated by numerical experiments. This example gives evidence that the two-scale expansion may be clearly superior to the regular expansion under certain circumstances like the appearance of secular terms.

4.3 Additional cubic time scale

Now let us look what happens with the multiscale expansion if we set $\omega = 2$. In this case the diffusivity coefficient $\mu = (\frac{1}{\omega} - \frac{1}{2})(1 - a^2)$ becomes 0. So the diffusion equation in (44) degenerates to $\partial_{t_2} u^{(0)} = 0$ implying that $u^{(0)}$ is not dependent on t_2 at all. Taking the initial condition $u^{(0)}(0, 0, x) = v_0(x)$ and the advection equation into account this amounts to $u^{(0)}(t_1, t_2, x) = v_0(x - at_1)$. Thus $u^{(0)}$ does not capture a damping exponential factor, that could guarantee the uniform boundedness of the $u^{(\beta)}$'s with respect to the t_2 similarly to the example d in the preceding subsection. Computing $u^{(1)}(t_1, t_2, x) = t_2 \lambda v_0'''(x - at_1)$ we see that it gets unbounded for $t_2 \to \infty$. Hence the two-scale expansion with the additional quadratic time scale is not able to avoid secular terms.

In subsection 4.1, we have noticed (cf. figure 3), that for $\omega = 2$ oscillations emerge and modify themselves in the cubic time scale. This suggests to approximate the population function by a prediction function $\mathsf{f}^{[\alpha]}(t_1, t_3, x)$ having two time arguments as well, but with the second one differently related to the n^{th} iteration:

$$\mathsf{F}(nh, jh) \approx \mathsf{f}(nh, nh^3, jh) \qquad \text{or} \qquad \mathsf{F}(t, x) \approx \mathsf{f}(t, h^2 t, x).$$

In order to keep this slight modification with respect to (40) in mind, we have denoted the second temporal argument by t_3. Again we choose for f the ansatz of a polynomial $\mathsf{f}^{[\alpha]}$ of order α in h. Then, under analogous assumptions as in the previous subsection, we can derive the following equations for $\alpha \geq 4$ to determine the leading asymptotic order functions.

$$\left.\begin{aligned}
h^0 &: \mathsf{f}^{(0)} && = (I + J)\mathsf{f}^{(0)} \\
h^1 &: \mathsf{f}^{(1)} + D\mathsf{f}^{(0)} && = (I + J)\mathsf{f}^{(1)} \\
h^2 &: \mathsf{f}^{(2)} + D\mathsf{f}^{(1)} + \tfrac{1}{2}D^2\mathsf{f}^{(0)} && = (I + J)\mathsf{f}^{(2)} \\
h^3 &: \mathsf{f}^{(3)} + D\mathsf{f}^{(2)} + \tfrac{1}{2}D^2\mathsf{f}^{(1)} + \tfrac{1}{6}D^3\mathsf{f}^{(0)} + \partial_{t_3}\mathsf{f}^{(0)} && = (I + J)\mathsf{f}^{(3)} \\
h^4 &: \mathsf{f}^{(4)} + D\mathsf{f}^{(3)} + \tfrac{1}{2}D^2\mathsf{f}^{(2)} + \tfrac{1}{6}D^3\mathsf{f}^{(1)} + \tfrac{1}{24}D^4\mathsf{f}^{(0)} + \partial_{t_3}\mathsf{f}^{(1)} + D\partial_{t_3}\mathsf{f}^{(0)} && = (I + J)\mathsf{f}^{(4)}
\end{aligned}\right\}. \quad (48)$$

Similarly to the procedure in 3.1 and 4.2, these equations are written in terms of the mass moments associated to the asymptotic order functions

$$\left.\begin{aligned}
(48_1) \quad &\Rightarrow \quad \partial_{t_1} u^{(0)} + a\partial_x u^{(0)} = 0 \\
(48_2) \quad &\Rightarrow \quad \partial_{t_1} u^{(1)} + a\partial_x u^{(1)} = 0 \\
(48_3) \quad &\Rightarrow \quad \partial_{t_1} u^{(2)} + a\partial_x u^{(2)} = \tilde{\lambda}\partial_x^3 u^{(0)} - \partial_{t_3} u^{(0)} \\
(48_4) \quad &\Rightarrow \quad \partial_{t_1} u^{(3)} + a\partial_x u^{(3)} = \tilde{\lambda}\partial_x^3 u^{(1)} - \partial_{t_3} u^{(1)}
\end{aligned}\right\} \quad (49)$$

where $\tilde{\lambda} := -\frac{1}{6}a(1-a^2)$ shortcuts the coefficient λ for $\omega = 2$. Splitting (49_3) into separate equations for the left and right hand side we get a complete[21] set of equations for $u^{(0)}$.

$$\boxed{\begin{array}{rcrcl} \partial_{t_1} u^{(0)}(t_1,t_3,x) & + & a\partial_x u^{(0)}(t_1,t_3,x) & = & 0 \\ \partial_{t_3} u^{(0)}(t_1,t_3,x) & - & \tilde{\lambda}\partial_x^3 u^{(0)}(t_1,t_3,x) & = & 0 \\ \multicolumn{5}{c}{u^{(0)}(0,0,x) = v_0(x)} \end{array}} \tag{50}$$

Moreover, combining (49_2) and (49_4) we find in the same way:

$$\boxed{\begin{array}{rcrcl} \partial_{t_1} u^{(1)}(t_1,t_2,x) & + & a\partial_x u^{(1)}(t_1,t_2,x) & = & 0 \\ \partial_{t_3} u^{(1)}(t_1,t_2,x) & - & \tilde{\lambda}\partial_x^3 u^{(1)}(t_1,t_3,x) & = & 0 \\ \multicolumn{5}{c}{u^{(1)}(0,0,x) = 0} \end{array}} \tag{51}$$

The second equation of (50) states that the dynamics of $u^{(0)}$ in the slow time variable is described by a *dispersive* equation. A characteristic property of this equation is to disperse a peak into a sequence of oscillations similarly to what we have observed (cf. figure 3). The reason for this behavior is found if we study the evolution of a single Fourier mode. Let us therefore consider a sinusoidal initial condition:

$$v_0(x) = \cos(2\pi m x).$$

Integrating the dispersion equation in (50) with this initialization yields

$$u^{(0)}(0,t_3,x) = \cos\left(8\pi^3 m^3 \tilde{\lambda} t_3 + 2\pi m x\right). \tag{52}$$

Differently from the diffusion equation, the sinusoidal profile is transported and not damped. In contrast to the advection equation which conserves the initial profile the transport velocity depends on the spatial frequency of the cosine. Hence the Fourier modes of an arbitrary initial profile travel with different speeds. This effect destroys the original shape of the profile.
Taking (52) as initial condition for the advection equation in (50) yields the final result for $u^{(0)}$.

$$\boxed{u^{(0)}(t_1,t_3,x) = \cos\left(8\pi^3 m^3 \tilde{\lambda} t_3 + 2\pi m(x - a t_1)\right)}$$

Let us now turn to (51) that differs from the analogous equations (21) and (45), because of the missing source term. Due to the zero initial condition $u^{(1)}$ must vanish.

$$\boxed{u^{(1)}(t_1,t_3,x) = 0}$$

Thus, the asymptotic expansion of the mass moment omits the first order for $\omega = 2$, wherefore the lattice Boltzmann scheme reaches higher accuracy in this case as mentioned earlier in subsection 3.3.

[21] Observe that we must expand up to the third order to extract the full set of evolution equations determining $u^{(0)}$.

How does the expansion continue? In general the second order $u^{(2)}$ does not vanish. Due to the resonance effect[22] it will be of the form $t_3 w(t_1, t_3, x)$ with some function w. Resubstituting t_1 by t and t_3 by $h^2 t$ produces a factor h^4 in front of $u^{(2)}$. This indicates that $u^{(0)}$ should approximate the mass moment U up to a residue of magnitude $\mathrm{O}(h^4)$ over time intervals of constant length. This hypothesis is supported by numerical tests. The approximation order is reduced by 1 and 2 respectively if we couple the number of iterations quadratically or cubically to the inverse of the grid spacing h (time intervals of length $\mathrm{O}(h^{-2})$ or $\mathrm{O}(h^{-3})$).

To better understand how the particularity of the missing first order comes about, let us close this subsection by delivering the computation in detail:

In order to obtain (49_3) and from this (51) we must take the scalar product of (48_4) with $\mathsf{1}$. Since

$$\langle J\mathsf{f}^{(4)}, \mathsf{1}\rangle = 0, \qquad \text{and} \qquad \langle D\partial_{t_3}\mathsf{f}^{(0)}, \mathsf{1}\rangle = \partial_{t_3}\langle D\mathsf{f}^{(0)}, \mathsf{1}\rangle = \partial_{t_3}(\partial_t u^{(0)} + a\partial_x u^{(0)}) = 0$$

we get

$$0 = \overbrace{\langle \partial_{t_3}\mathsf{f}^{(1)}, \mathsf{1}\rangle}^{=\partial_{t_3} u^{(1)}} + \overbrace{\langle D\,\mathsf{f}^{(3)}, \mathsf{1}\rangle + \tfrac{1}{2}\langle D^2\mathsf{f}^{(2)}, \mathsf{1}\rangle + \tfrac{1}{6}\langle D^3\mathsf{f}^{(1)}, \mathsf{1}\rangle + \tfrac{1}{24}\langle D^4\mathsf{f}^{(0)}, \mathsf{1}\rangle}^{=:A}.$$

It remains to compute A. Applying D^4, D^3, D^2 and D to (48_{1-3}) and taking the scalar product with $\mathsf{1}$ yields the following identities

$$\begin{aligned}
\langle D\ \mathsf{f}^{(3)}, \mathsf{1}\rangle &= \langle D\ \mathsf{E}^{(3)}, \mathsf{1}\rangle - \tfrac{1}{\omega}\langle D^2\mathsf{f}^{(2)}, \mathsf{1}\rangle - \tfrac{1}{2\omega}\langle D^3\mathsf{f}^{(1)}, \mathsf{1}\rangle - \tfrac{1}{6\omega}\langle D^4\mathsf{f}^{(0)}, \mathsf{1}\rangle \\
\langle D^2\mathsf{f}^{(2)}, \mathsf{1}\rangle &= \langle D^2\mathsf{E}^{(2)}, \mathsf{1}\rangle - \tfrac{1}{\omega}\langle D^3\mathsf{f}^{(1)}, \mathsf{1}\rangle - \tfrac{1}{2\omega}\langle D^4\mathsf{f}^{(0)}, \mathsf{1}\rangle \\
\langle D^3\mathsf{f}^{(1)}, \mathsf{1}\rangle &= \langle D^3\mathsf{E}^{(1)}, \mathsf{1}\rangle - \tfrac{1}{\omega}\langle D^4\mathsf{f}^{(0)}, \mathsf{1}\rangle \\
\langle D^4\mathsf{f}^{(0)}, \mathsf{1}\rangle &= \langle D^4\mathsf{E}^{(0)}, \mathsf{1}\rangle
\end{aligned}$$

where we have once again used $\langle D\partial_{t_3}\mathsf{f}^{(0)}, \mathsf{1}\rangle = 0$ for the first equation and $J\mathsf{f}^{(\beta)} = \omega\mathsf{E}^{(\beta)} - \omega\mathsf{f}^{(\beta)}$. Thereby we get for A:

$$\begin{aligned}
A &= \langle D\mathsf{f}^{(3)}, \mathsf{1}\rangle + \tfrac{1}{2}\langle D^2\mathsf{f}^{(2)}, \mathsf{1}\rangle + \tfrac{1}{6}\langle D^3\mathsf{f}^{(1)}, \mathsf{1}\rangle + \tfrac{1}{24}\langle D^4\mathsf{f}^{(0)}, \mathsf{1}\rangle \\
&= \langle D\mathsf{E}^{(3)}, \mathsf{1}\rangle + \underbrace{(\tfrac{1}{2} - \tfrac{1}{\omega})}_{=0 \text{ for } \omega=2}\langle D^2\mathsf{f}^{(2)}, \mathsf{1}\rangle + (\tfrac{1}{6} - \tfrac{1}{2\omega})\langle D^3\mathsf{f}^{(1)}, \mathsf{1}\rangle + (\tfrac{1}{24} - \tfrac{1}{6\omega})\langle D^4\mathsf{f}^{(0)}, \mathsf{1}\rangle \\
&= \langle D\mathsf{E}^{(3)}, \mathsf{1}\rangle + (\tfrac{1}{6} - \tfrac{1}{2\omega})\langle D^3\mathsf{E}^{(1)}, \mathsf{1}\rangle + \big[(\tfrac{1}{24} - \tfrac{1}{6\omega}) - \tfrac{1}{\omega}(\tfrac{1}{6} - \tfrac{1}{2\omega})\big]\langle D^4\mathsf{f}^{(0)}, \mathsf{1}\rangle \\
&= \langle D\mathsf{E}^{(3)}, \mathsf{1}\rangle + \underbrace{(\tfrac{1}{6} - \tfrac{1}{2\omega})}_{=-1/12 \text{ for } \omega=2}\langle D^3\mathsf{E}^{(1)}, \mathsf{1}\rangle + \underbrace{\big[\tfrac{1}{24} - \tfrac{1}{3\omega} + \tfrac{1}{2\omega^2}\big]}_{=0 \text{ for } \omega=2}\langle D^4\mathsf{f}^{(0)}, \mathsf{1}\rangle \\
&= \langle D\mathsf{E}^{(3)}, \mathsf{1}\rangle - \tfrac{1}{12}\langle D^3\mathsf{E}^{(1)}, \mathsf{1}\rangle
\end{aligned}$$

[22] Generally: If A is some (linear, spatial differential) operator and $x(t,\cdot)$ a solution of the homogeneous equation $\partial_t x + Ax = 0$ then $y(t,\cdot) = tx(t,\cdot)$ is a solution of the inhomogeneous equation $\partial_t y + Ay = x$. So the solution of the equation (describing the behavior of some physical system) imitates (reacts like) the source while amplified in time due to the multiplication with t. This phenomenon is called *resonance*. Moreover, y becomes unbounded if x does not decay faster to 0 than $1/t$ as $t \to \infty$ (resonance catastrophe).

Concretely: The dispersive equations arising in the asymptotic orders do not differ in the main part (equal dispersion coefficient $\tilde{\lambda}$) but only in the source terms, that are solutions of lower order dispersive equations. Therfore the solutions contain powers of t_3 as factors. Since there is no exponential damping as in the case of the diffusion equation we expect the expansion to produce secular terms too similarly to the case of the advection equation (regular expansion) but in a much slower time scale.

Next, we employ $\langle D\mathsf{E}^{(3)}, \mathsf{1}\rangle = \partial_{t_1} u^{(3)} + a\partial_x u^{(3)}$ and

$$\langle D^3\mathsf{E}^{(1)}, \mathsf{1}\rangle = \tfrac{1}{2}\big\langle(\partial_{t_1}^3 + 3\mathsf{s}\partial_{t_1}^2\partial_x + 3\partial_{t_1}\partial_x^2 + \mathsf{s}\partial_x^3)(1+a\mathsf{s})u^{(1)}, \mathsf{1}\big\rangle = -2a(1-a^2)\partial_x^3 u^{(1)}$$

where the latter formula holds true as $u^{(1)}$ also solves the homogeneous advection equation. Thus, we finally arrive at

$$\partial_{t_3} u^{(1)} + \partial_{t_1} u^{(3)} + a\partial_x u^{(3)} - \tfrac{1}{12}\big(-2a(1-a^2)\big)\partial_x^3 u^{(1)} = 0$$

which is equivalent to (49_3).

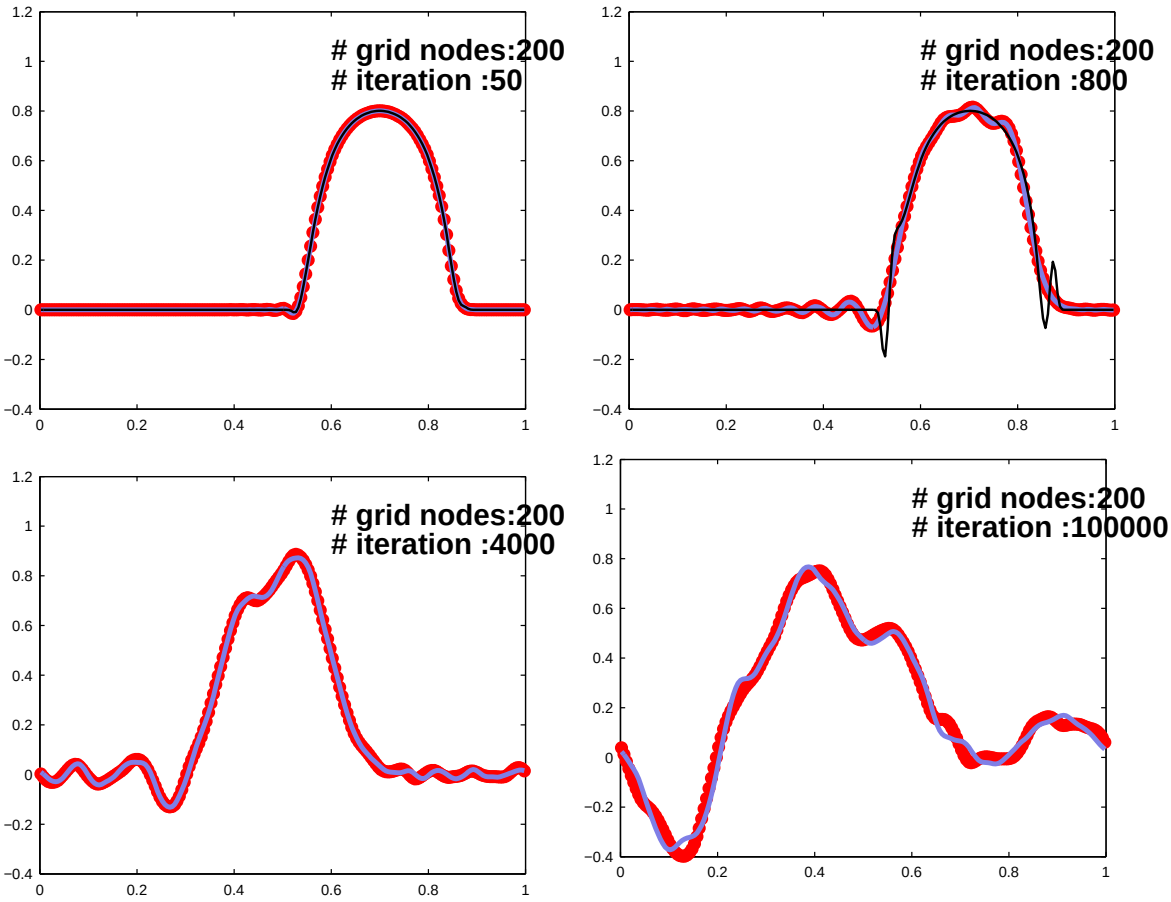

Figure 4:
The figure shows four snapshots of the mass moment $U(nh,\cdot)$ (gray dashed). The thin solid line indicates the prediction $u^{(0)}(nh,\cdot)+hu^{(1)}(nh,\cdot)+h^2u^{(2)}(nh,\cdot)$ obtained by the *regular* expansion. In contrast, the black dashed line refers to the prediction $u^{(0)}(nh,nh^3,\cdot)$ that results from the *multiscale* expansion.
After 50 iterations ($t=0.25$) the initial profile is shifted rightwards by 0.2 length units ($a=0.8$); the distortion is hardly visible. 750 iterations later ($t=4$) the distortion becomes noticeable. The regular expansion displays serious problems at the two knees where very sharp peaks are formed that evoke a certain similarity to the second and third derivative of the initial profile (see figure 5). Due to the secular terms in the regular expansion the derivatives of the initial profile are amplified in time, what makes the peaks grow quickly outside the range of the coordinate system. While the multiscale prediction imitates the oscillations of U very well even after 100000 iterations, the resemblance between U and the regular prediction is lost.

5 Appendix

Here we give the analytic description of the bump-like test profile that we have used as initial condition to illustrate the cubic time scaling (cf. figure 3) and to validate

the two-scale expansion with cubic time (cf. figure 4).

$$\phi(x) := \begin{cases} x \leq 0.3 & : \quad 0 \\ 0.3 < x < 0.7: & \exp\left(\frac{-15^{-2}}{\left((x+0.2)-0.5\right)^2}\right) \cdot \exp\left(\frac{-15^{-2}}{\left((x-0.2)-0.5\right)^2}\right) \\ 0.7 \leq x & : \quad 0 \end{cases}$$

The function ϕ is arbitrarily smooth (no kinks) but not analytic. Note that each

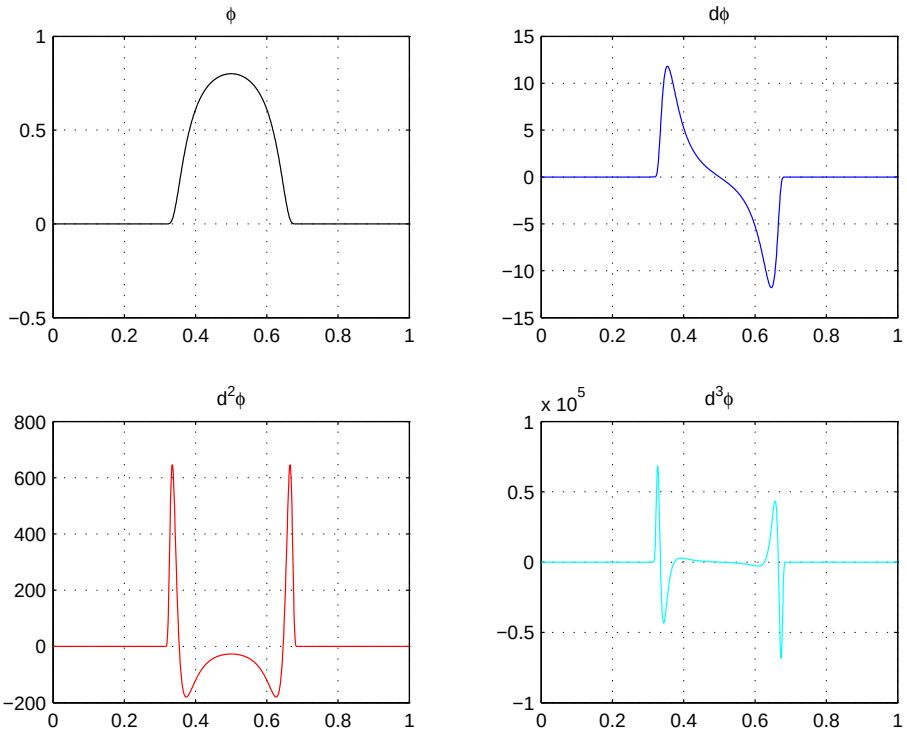

Figure 5:
Left above: Test profile for initializing the mass moment. The other figures display the first, second and third spatial derivative. Compare the orders of magnitude concerning the scaling of the ordinates.

derivative is at least one order of magnitude larger than the previous one. This explains why the regular expansion containing higher order derivatives 'explodes' rapidly. Furthermore ϕ is identically zero outside of the bump, which means that all derivatives vanish there too. By this reason the regular expansion has no chance even rudimentarily to mimick the oscillations in figure 3 that fill the whole interval.

The computation of the two-scale prediction for the mass moment in figure 4 is based on a Fourier decomposition of ϕ.

References

[1] A. Caiazzo. Analysis of lattice Boltzmann initialization routines. *J. Stat. Phys.*, 121:37–48, 2005.

[2] M. Junk, A. Klar, and L.S. Luo. Asymptotic analysis of the lattice Boltzmann equation. *Journal Comp. Phys.*, 210:676–704, 2005.

[3] M. Junk and Z. Yang. Analysis of lattice Boltzmann boundary conditions. *Proc. Appl. Math. Mech.*, 3:76–79, 2003.

[4] M. Junk and Z. Yang. Asymptotic analysis of finite difference methods. *Appl. Math. Comput.*, 158:267–301, 2004.

[5] M. Junk and Z. Yang. Asymptotic analysis of lattice Boltzmann boundary conditions. *J. Stat. Phys.*, 121:3–35, 2005.

[6] M. Junk and Z. Yang. One-point boundary condition for the lattice Boltzmann model. *Phy. Rev. E*, 72, 2005.

[7] M. Rheinländer. A consistent grid coupling method for lattice-Boltzmann schemes. *J. Stat. Phys.*, 121:49–74, 2005.